Yb^{3+} Concentration Effects in Novel Yb Doped Lanthano-Alumino-Silicate Fibers: Experimental Study

Alexander V. Kirýanov, *Member, IEEE*, Mukul Chandra Paul, *Member, IEEE*, Yuri O. Barmenkov, *Member, IEEE*, Shyamal Das, Mrinmay Pal, and Luis Escalante-Zarate

***Abstract*— Novel lanthano-alumino-silicate optical fibers doped with ytterbium (Yb) in a wide concentration range are obtained through the conventional modified chemical vapor deposition process and solution doping technique. The featuring fibers' characteristics are determined, applying a routine that involves the spectroscopic, nonlinear-optical, and laser methods as well as photodarkening tests. Special attention is paid to address thoroughly the effect of Yb^{3+} concentration upon the fibers' properties.**

***Index Terms*— Yb-doped fibers, optical fiber characterization, nonlinear refractive index, nonlinear transmission coefficient, laser dynamics, photodarkening, Yb_2O_3.**

I. Introduction

CURRENTLY, considerable work is carried out on the incorporation of Yb^{3+} dopants into different fiber core glasses for inspecting their potential for laser applications. The main target at this is keeping high optical efficiency of an Ytterbium (Yb) doped fiber system, the highest as compared to other rare-earth doped ones, and in the meantime diminishing photodarkening (PD), a detrimental effect known as seriously deteriorating output characteristics of fiber lasers and amplifiers. For instance, we recently attempted to approach these goals by fabricating and investigating a row of novel Yb doped fibers [1]–[3].

As a continuation of the research, we found interesting to develop and study one more type of Yb doped fibers based on lanthano-alumino-silicate (LAS) glass. So far, the LAS-Yb system is poorly known: Only a few studies have been published on the theme; see Refs. [4]–[8]. Among them, the basic properties of pure bulk LAS glass were studied in Ref. [4] and some aspects of LAS glasses, also bulk, codoped with Yb^{3+}/Ho^{3+} and Yb^{3+}/Tm^{3+} were inspected [5], [6] towards optimization of energy transfer from Yb^{3+} to Ho^{3+}/Tm^{3+} for 2-μm lasing. One more work concerning optical properties of Lanthanum (La) and Yb codoped tellurite glass was published recently [7] where the glass properties associated with the presence of La are discussed. Only a single research [8] published a few years back dealt with LAS-Yb fibers as promising for lasing at 980 nm, given by opportunity to make-up high numerical aperture (NA) in such fibers. To the best of our knowledge, no more researches on the matter were done to date. In virtue of this, i.e. because of a very little knowledge about LAS-Yb based optical fibers, we believe that our present report would have a value.

In the LAS glass, La-O bonds are stronger because of the high field-strength of La^{3+} ions and so such glasses exhibit high glass transition temperatures that range from 800 to 900°C and are virtually independent of composition. The excellent physical properties and lower optical basicity make LAS glasses and fibers on their base potential hosts for Yb^{3+} doping. Furthermore, a small amount of Li introduced in our LAS-Yb fibers (see below) provides glass-ceramic based phase-separated nano-sized zones, which shield the Yb^{3+} ions from the bulk glass of high-phonon energy in a local environment, allowing high thermal stability during high-power applications.

The LAS-Yb fibers, doped with Yb in a wide concentration range, were obtained through the conventional modified chemical vapor deposition (MCVD) process and solution doping (SD) technique. The fabricated fibers were then explored through a set of characterization procedures that included the measurements of absorption and fluorescence spectra and Yb^{3+} fluorescence lifetimes as well as laser and PD tests, upon 976-nm pumping. We also made insight to the nonlinear-optical properties of the LAS-Yb fibers in terms of nonlinear transmission coefficient and nonlinear refractive index, both obtained at resonant (into Yb^{3+} band) excitation.

Throughout the characterization route, we paid the most of attention to the factor of Yb^{3+} concentration, which affects almost all optical parameters of the LAS-Yb fibers, sometimes useful or harmful for applications. This, in the meantime, allowed us to reveal certain general aspects of Yb doped

Manuscript received September 7, 2012; revised March 13, 2013; accepted April 10, 2013. Date of publication April 19, 2013; date of current version May 2, 2013. This work was supported in part by through the Programme of Cooperation in Science & Technology between Mexico (CONACYT) and India (DST).

A. V. Kirỳanov, Y. O. Barmenkov, and L. Escalante-Zarate are with the Centro de Investigaciones en Optica, Leon 37150, Mexico (e-mail: kiryanov@cio.mx; yuri@cio.mx; itrio@cio.mx).

M. C. Paul, S. Das, and M. Pal are with the Fiber Optics and Photonic Division, Central Glass & Ceramic Research Institute (CSIR-CGCRI), Kolkata 700 032, India (e-mail: mcpal@cgcri.res.in; mpal@cgcri.res.in; dshyamal@cgcri.res.in).

Color versions of one or more of the figures in this paper are available online at http://ieeexplore.ieee.org.

Digital Object Identifier 10.1109/JQE.2013.2259143

fibers regarding the Yb^{3+} concentration effect, important for practice.

II. Fiber Preforms Fabrication and Characterization

Doping the core silicate glass with glass modifiers Al_2O_3, Li_2O, La_2O_3, and Yb_2O_3 was done through the SD process. It is known that fluorescent properties of rare-earth ions strongly depend on phonon frequency of the host; thus, a low phonon energy of La_2O_3 (around 400 cm^{-1}) was expected to be a good choice for getting highly fluorescing LAS-Yb based fibers – see e.g. Ref. [7], [8]. The other advantage of La_2O_3 oxide is its low cost compared with other rare-earth glass modifiers such as Y_2O_3, Gd_2O_3 *etc.* Co-doping with La (as well as with Lithium) is also attractive for enhancing transparency of the core glass and reducing optical loss. Among other details concerning making-up of the LAS-Yb glass, mention that the glass former SiO_2 was incorporated by means of vapour phase deposition and that a small amount, ~0.05–0.1 mol.%, of P_2O_5, a nucleating agent, was added to facilitate phase separation with formation of silica-rich and silica-deficiency zones in the glass.

Fabricating of the LAS-Yb fiber preforms had the following steps and technological details. A single porous layer of phospho-silicate glass was deposited within the inner surface of a silica tube with outer/inner diameters of 20 / 17 mm at the optimum deposition temperature, 1475±25°C, with flow of mixture of $SiCl_4$, $POCl_3$, O_2, and He gases, followed by pre-sintering for one pass at temperatures 1400–1450°C. Soaking of the porous soot layer was done into a solution of alcoholic-water (1:5) mixture of suitable strength of $YbCl_3.6H_2O$, $AlCl_3.6H_2O$, $LaCl_3.7H_2O$, and $LiNO_3$ for 1 hour. The single-pass pre-sintering was undertaken for making good adhesion of the deposited porous layer with inner silica surface in order to prevent disturbances during the solution soaking period, using suitable strength of the dopants' precursors. After draining out the solution, the layer containing Yb, La, and Al salts was dried with flow of N_2 gas at room temperature for 30 minutes and then – dried thermally by heating at about 1100–1200°C with flows of O_2 (at the rate of 500 cc/min) and He (at the rate of 75–100 cc/min) gases for the salts' oxidation. Dehydration of the core layer was carried out within a temperature range 800–1100°C in the presence of mixture of Cl_2 and O_2 gases at a Cl_2:O_2 ratio ranged from 1.5:1 to 3:1. Sintering of the core layer was done with flow of gaseous mixture of 80% O_2 and 20% He at temperatures ranged from 1300 to 1900°C by a step-wise increment by 100°C. After complete sintering, the tube was collapsed with flow of gaseous mixture of 90–95% O_2 and 10–5% He at a temperature between 2000 and 2300°C to obtain a preform. The tube was collapsed in 3 to 4 burner's passes at temperatures above 2000°C; the burner's traverse speed was gradually decreased from 4 to 2 cm/min in subsequent passes. Deposition of the porous core layer, drying of the soaked layer, sintering, and collapsing were made under highly oxidizing atmosphere to reduce the formation of such unwanted defects as aluminium-related oxygen-hole centers (Al-OHC). This procedure allowed us to reach the optimal

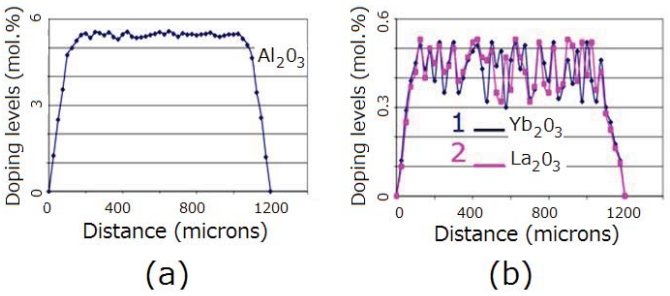

Fig. 1. The distributions of doping levels of (a) Al_2O_3 and (b) Yb_2O_3 (curve 1) / La_2O_3 (curve 2) across the core area of the LAS-Yb fiber preform from which YbLa-3 fiber (see below) was drawn [EPMA data].

preforms' parameters, targeted on final LAS-Yb based fibres with NA around 0.2. Such LAS-Yb fibers were drawn using a standard drawing tower at a temperature around 2000°C.

The compositions and the dopants' average molar weights and their radial distributions in preforms were measured using an electron probe micro analysis (EPMA). The featuring dopants' distributions in one of the fabricated preforms are demonstrated in Fig. 1. It is seen from the figure that the dopants are distributed uniformly through the whole core area.

The refractive index (RI) profiles of three preforms with different Yb^{3+} concentrations, from which the final fibers (YbLa-3, YbLa-4, and YbLa-5) were drawn, are shown on the right side of Fig. 2 (column b); these were measured using a fiber analyzer. It is seen that RI profiles are very sharp at the core-cladding boundary; the sharpness most probably indicates that the doping elements are embedded entirely within the core regions of the preforms.

A TEM analysis has revealed that the fiber preforms exhibit phase separation near the core-cladding interface (see Fig. 3), the fact that also has impact on sharpness of the RI profiles.

It is known that phase separation gives rise to scattering of the higher-order modes in a fiber and their effective extinguishing. Thus, these modes should "see" a much greater attenuation at propagating along the fiber whereas the lower-order ones, confined within the central core region, should not experience such scattering and "see" less attenuation. Thereafter, the higher-order modes' attenuation will effectively reduce NA and severely impact the coupling efficiency [9]. This effect was observed at experimenting with final LAS-Yb fibers: In short-length fiber cutbacks, a far-field divergence angle becomes length-dependent, confirming the modal selection, an interesting property of the fibers.

On the other hand, the immiscibility gap in rare-earth alumino-silicates is also known. The gap extends from 80 to 90 mol.% of SiO_2 at the Al_2O_3:RE_2O_3 ratio of about 2.5:1 and extends much further on the RE_2O_3 rich-side; this compositional region is deep within the immiscibility gap mapped in Ref. [10], which extends from 75 to 98% SiO_2 when the Al_2O_3:RE_2O_3 ratio is 1, so phase separate along the interface on cooling. To eliminate the problem of immiscibility, glasses richer in Al_2O_3 have been made (see Table I). At an Al_2O_3:RE_2O_3 ratio of 2.3–2.5, the immiscibility gap is minimized [11]. In addition, the kinetics of phase separation

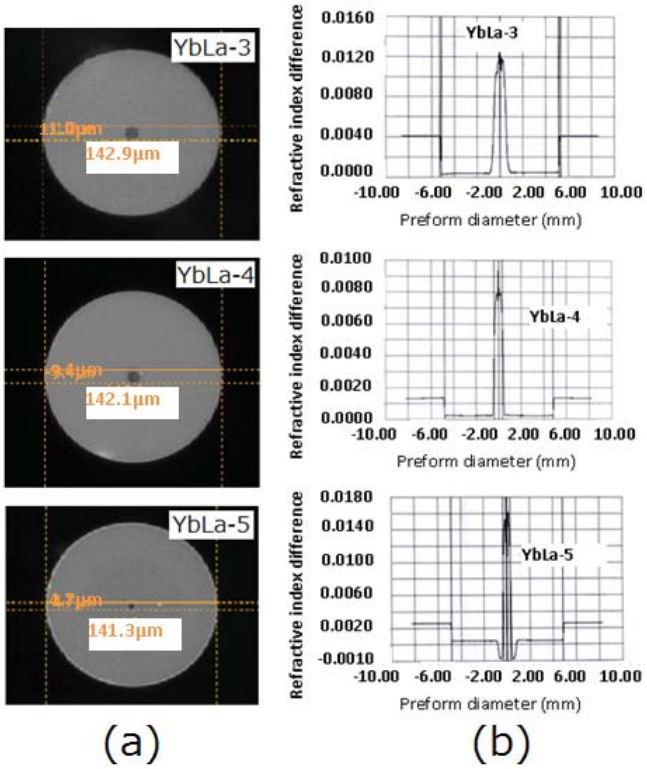

Fig. 2. (a) Photos of cleaved ends of the final LAS-Yb fibers [optical microscopy data]. (b) RI profiles of the sourcing LAS-Yb preforms [fiber analyzer data].

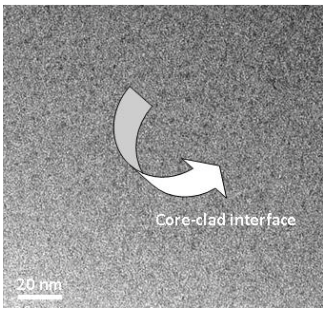

Fig. 3. TEM picture of the preform from which YbLa-3 fiber was drawn (a 20-nm scale). The arrow allocates the core-clad phase-separated interface area.

was also found to be much slower in the LAS-Yb glasses, since the separation does not occur until higher SiO_2 contents.

III. Optical Properties of Final Fibers

We examine next the spectroscopic, nonlinear-optical, and laser properties of the drawn fibers, labeled further YbLa-3, YbLa-4, and YbLa-5.

The essential parameters' values of the fibers are given in Table I and the microscopic pictures of their cross-sectional areas are shown on the left side of Fig. 2 (column a); these data were collected using an optical microscope of the Vytran's equipment.

The fibers were found to be easily and low-loss spliced with standard single-mode silica fibers, owing to similarity in the melting temperatures of these two kinds of fiber.

TABLE I
Parameters of the Fabricated LAS-Yb Fibers

Fiber ##	Core Composition	Core Dia. μm	NA	Overlap Factor	Mode Dia. μm	Yb^{3+} Content $cm^{-3} \times 10^{-20}$ [Estimate]
YbLa-3	SiO_2-Li_2O+Al_2O_3-La_2O_3-Yb_2O_3 Al_2O_3:- 5.5 mol.% La_2O_3: 0.45 mol.% Yb_2O_3:-0.45 mol.%	11.0	0.19	0.95	8.2	0.80
YbLa-4	SiO_2-Li_2O+Al_2O_3-La_2O_3-Yb_2O_3 Al_2O_3:- 5.0 mol.% La_2O_3: 0.45 mol.% Yb_2O_3:-0.75 mol.%	9.4	0.15	0.97	7.7	1.71
YbLa-5	SiO_2-Li_2O+Al_2O_3-La_2O_3-Yb_2O_3 Al_2O_3:- 7.0 mol.% La_2O_3: 0.45 mol.% Yb_2O_3: 0.1 mol.%	4.7	0.22	0.91	4.3	0.07

A. Absorption Spectra

The absorption spectra of YbLa-3, YbLa-4, and YbLa-5 fibers are presented in Fig. 4. Experimentally, the spectra shown in Figs. 4(a)–(c) were obtained using a white-light source with fiber output as probe and an optical spectrum analyzer (OSA) with a 0.2–0.5 nm resolution.

It is seen that the spectra are quite similar in the appearance for all three fibers, differing in the Yb^{3+} peaks extinction mainly: The absorption coefficients at 976 nm of YbLa-4, YbLa-3, and YbLa-5 fibers were measured to be 1220, 610, and 30 dB/m, respectively (Fig. 4(a)). The basic idea to fabricate LAS-Yb fibers with such attenuations (the heavily doped YbLa-4 and YbLa-3 fibers differ twice in Yb^{3+} concentration and the weakly doped YbLa-5 one is a reference) was to inspect the effect of Yb^{3+} concentration upon the fibers' key optical properties.

Note that the peaks within the resonant-absorption band of Yb^{3+} (nearby 915–920, 976, and 1020 nm – see arrows in Fig. 4(a)) are well resolved, in contrast to standard alumino-silicate fibers free from La and Li. This and also the fact that the zero-phonon peak of the LAS-Yb fibers (at 976 nm) is quite narrow (measured by 6–6.5 nm), can be explained by the role of La as a strong modifier of the core glass (remind that La_2O_3 has a low phonon frequency, about 400 cm^{-1}, which gives rise to lowering influence of the phonon system as the whole upon the optical properties of LAS-Yb glass).

In accordance to Fig. 4(a), a tentative scheme of the Yb^{3+} energy sublevels of $^2F_{7/2}$ and $^2F_{5/2}$ manifolds is sketched in inset to the figure. The (a-a') transition corresponds to the most intensive and narrow (zero-phonon) peak at 976 nm, the (a-c') transition, also well resolved, is assigned as usually to absorption from the lowest ground-state sublevel to the highest sublevel of the excited state of Yb^{3+}, while the (b'-a') transition – to absorption from the second sublevel of the ground state of Yb^{3+}, which is partially thermally populated at room temperature. The transition (a-b'), similarly to other silica fibers, cannot be attributed from the absorption spectrum in Fig. 4(a), in contrast to phosphate fibers where this transition appears nearby 960 nm.

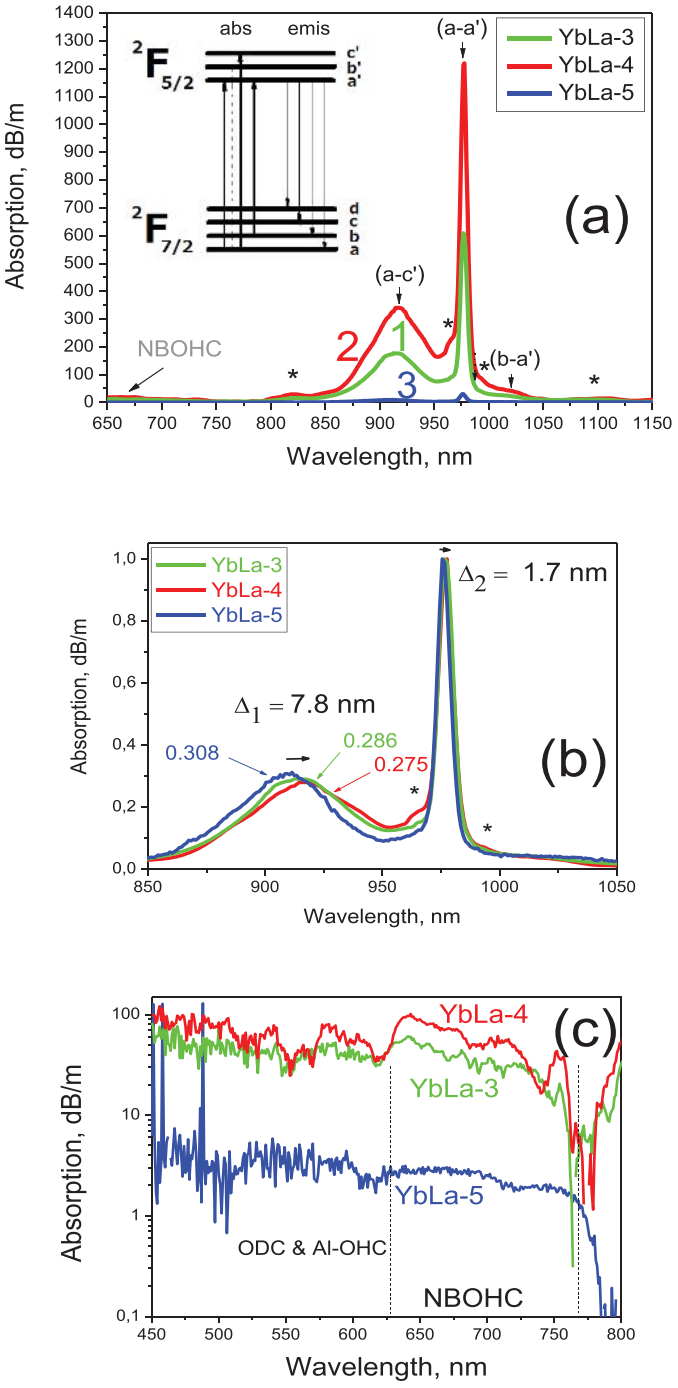

Fig. 4. (a) Attenuation spectra of YbLa-3 (curve 1), YbLa-4 (curve 2), and YbLa-5 (curve 3); (b) insight into the Yb^{3+} resonant band, showing re-distribution and shifting of Yb^{3+} peaks with increasing Yb^{3+} content in the LAS-Yb fibers; and (c) insight into VIS spectral range, showing an increase of loss due to the presence of NBOHC with increasing Yb^{3+} concentration.

We also mark by asterisks in Fig. 4(a) the smaller in magnitude absorption peaks which were detected only in the heavier doped with Yb fibers (YbLa-3 and YbLa-4) but not – in the low-doped (YbLa-5) one. Possible reasons for this shall be discussed further.

The two – also small but detectable – features can be seen from Fig. 4(b) where we show the normalized (on absorption coefficients α_0 at the 976-nm peak) spectra. Namely, one can

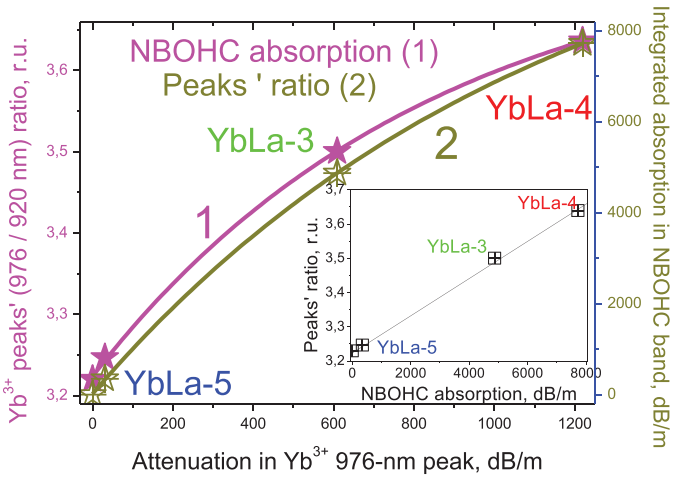

Fig. 5. The essences derived from Fig. 4(b) and (c), *i.e.* NBOHC absorption and ratio of extinction in Yb^{3+} peaks at 976 and 920 nm as functions of attenuation in 976-nm peak of Yb^{3+} (given by curves 1 and 2, respectively). Inset shows the data in a parametric form, demonstrating a linear dependence between them.

observe from this figure *(i)* a Stokes shift of the main Yb^{3+} peaks, measured to be a few nanometers at increasing Yb^{3+} concentration and *(ii)* redistribution between the peaks' (at around 915–920 and 976–977 nm) magnitudes: The higher Yb^{3+} concentration the more intensive is the peak at 976 nm relatively to the one at 915–920 nm.

One more feature to be mentioned, when analyzing in more details the fibers' absorption spectra towards shorter wavelengths (see Fig. 4(c)), is that the background loss level, from VIS to near-IR, correlates with the resonant-absorption Yb^{3+} peaks' intensities: The higher Yb^{3+} concentration the more pronounceable is attenuation in VIS. This background loss can be provisionally assigned to the presence in fibers of non-bridged oxygen hole centers (NBOHC: 600–750 nm) and, probably, oxygen-deficit (ODC) and Al-OHC centers, also characteristic for silica fibers [12], [13].

A rise of NBOHC contribution with increasing Yb^{3+} concentration, in terms of extinction in the zero-phonon peak at 976 nm, is clearly seen in Fig. 5 (curve 1). It is a natural situation when an increase of the doping level of glass by Yb^{3+} ions leads to an increase of NBOHCs number. Furthermore, in the same figure we plot a ratio of the two main absorption peaks of Yb^{3+} (at 976 and 915–920 nm) as a function of extinction in the highest (976-nm) one; see curve 2. The mentioned redistribution in amplitudes of the two peaks of Yb^{3+} can be even quantified: It exceeds 10%, a distinct, concentration-related, feature of the LAS-Yb fibers. Inset in Fig. 5 demonstrates a linear dependence between the first and the second (the loss ascribed to NBOHC defects in the fibers). Some more assertions regarding the Yb^{3+} concentration-related details in the absorption spectra of the heavily doped YbLa-3 and YbLa-4 fibers as compared to the reference lower doped YbLa-5 one are given in Section IV.

B. Fluorescence Spectra and Fluorescence Lifetimes

The Yb^{3+} fluorescence spectra and the fluorescence kinetics in the LAS-Yb fibers were measured at 976-nm excitation

using a standard 400-mW laser diode (LD) with fiber output. The LD's output fiber was spliced to a fiber isolator (supporting power of up to 1 W at ~1 μm), which, in turn, was spliced to a tested LAS-Yb fiber sample, angle-cleaved from the other side to prevent any feedback.

1) Fluorescence Spectra: The measurements of Yb^{3+} fluorescence spectra were made in the lateral arrangement where a fiber sample of 1.0–1.5 cm in length is in-core pumped and fluorescence is collected from its lateral side, using a multimode patchcord connected either with an OSA or photodetector. At collecting the spectra, the LD operated in CW regime. The results are shown by Fig. 6.

The fluorescence spectra in Fig. 6 comprise two bands: the first, at 900–1200 nm, where Yb^{3+} resonant peaks are located, which correspond to the transitions between the manifolds $^2F_{5/2}$ and $^2F_{7/2}$, see inset to Fig. 4(a), and the second, at 450–600 nm, where Yb^{3+}–Yb^{3+} "cooperative" emission is expected to exist. We found reasonable to present in each figure (a)–(c) the spectra obtained at a certain pump power (main frames) together with integrated powers within the Yb^{3+} and Yb^{3+}–Yb^{3+} fluorescence bands (insets).

Note that IR range of the fluorescence spectra, apparently stemming from the presence of Yb^{3+} ions, is similar to that observed in standard alumino-silicate, La- and Li- free, Yb-doped fibers. Furthermore, all three fibers YbLa-5, YbLa-3, and YbLa-4 are featured by quite low saturating parameters at 976 nm, as can be revealed from the right-hand insets in Fig. 6. Saturating pump powers and intensities were estimated to be $P_s \approx 5$ (YbLa-5) and 8 (YbLa-4 and YbLa-3) mW and $I_s \approx 30.9$ (YbLa-5), 16.2 (YbLa-4), and 15.3 (YbLa-3) kW/cm^2, respectively. However, the situation with saturating intensities is in reality more complicate; see e.g. the next part highlighting the nonlinear-optical properties of the fibers.

Certainly, the Yb^{3+} concentration effect affects the fluorescent properties of the LAS-Yb fibers. The higher Yb^{3+} concentration the more pronounced is the "cooperative" emission – compare the spectra in the sequence YbLa-5→YbLa-3→YbLa-4 and also refer to Fig. 4 where the absorptive properties of the fibers are provided. Though we assign here the emission of the LAS-Yb fibers in VIS as "cooperative", there is a dispute in the literature regarding its origin. In the meantime, the spectral features seen in Fig. 6(a) and (b) in VIS as we think are to be ascribed to the "cooperative" emission since no other spectral features were detected, which would originate, say, from traces of unwanted rare-earth dopants like Tm^{3+} and Er^{3+} [14].

The ratio of VIS to near-IR powers, obtained after integrating the spectra in Fig. 6(a)–(c) within the relevant wavelengths' domains and plotted as a function of attenuation in the zero-phonon peak of Yb^{3+} at 976 nm, is demonstrated in Fig. 6(d) as an illustration of how the Yb^{3+} concentration effect manifests itself in the fluorescent properties of the LAS-Yb fibers. One can resume from this figure that there is an almost quadratic increase of the ratio, given by strong enhancement of the "cooperative" emission, ascribed to the presence in a medium of Yb^{3+}–Yb^{3+} *clusters*.

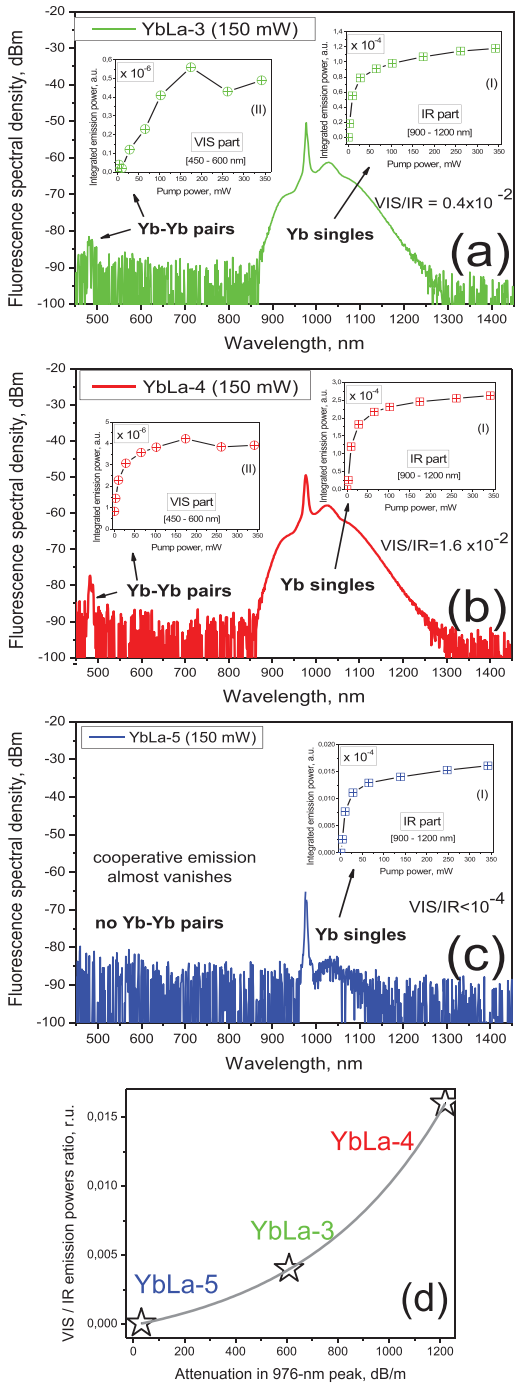

Fig. 6. Fluorescence spectra obtained for YbLa-3 (a), YbLa-4 (b), and YbLa-5 (c) fibers at pump power of 175 mW (main frames) and fluorescence saturation curves obtained at different pump powers (left insets in each figure — after integrating the spectra in the VIS range, 450–600 nm, and right insets in each figure — after integrating the spectra in the near-IR range, 900–1200 nm). Pump wavelength – 976 nm; spectral resolution – 0.5 nm. All the experiments were made at the same experimental conditions. (d) Ratios of VIS ("cooperative" emission) to near-IR ("fundamental" Yb^{3+} fluorescence) as a function of attenuation in 976-nm peak of Yb^{3+}, obtained from (a)–(c); plain curve is a fit of the data to guide the eye.

2) Fluorescence Lifetimes: In case of lifetime measurements, the same arrangement was employed but LD power was modulated by a driver controlled, in turn, by a function generator to achieve square-shape pulses of ms-width with

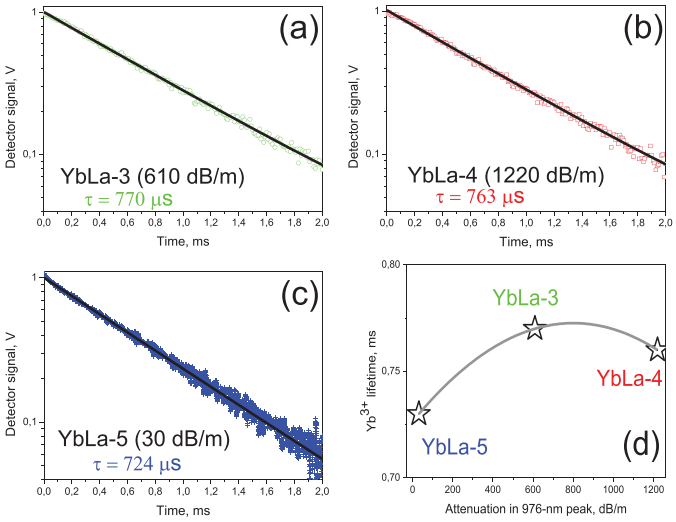

Fig. 7. Experimental fluorescence decays (symbols) of YbLa-3 (a), YbLa-4 (b), and YbLa-5 (c) after excitation at 976 nm (pump power – 150 mW). Plain curves are single-exponent fits of the data. (d) Yb^{3+} lifetime as a function of attenuation in 976-nm peak of Yb^{3+}, obtained from (a)–(c).

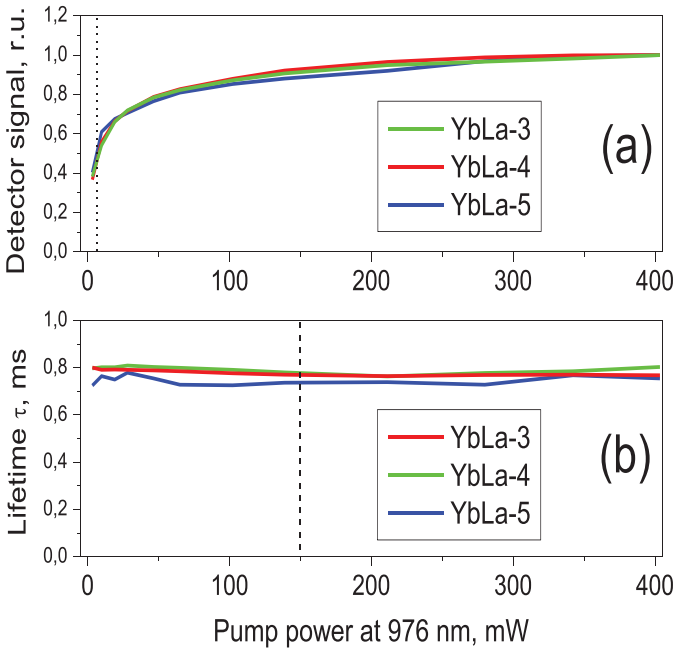

Fig. 8. Data obtained after processing the lifetime measurements for YbLa-3, YbLa-4, and YbLa-5 fibers. (a) Normalized fluorescence power measured with a photo-detector just before the modulator was switched off (characterizes the fluorescence saturation behavior) and (b) the correspondent fluorescence lifetime given by fits of decay kinetics. Both sets represent the dependences versus pump power at 976-nm wavelength. Vertical dashed line in figure (a) marks the saturating pump power (5…9 mW). Vertical dotted line in figure (b) shows the pump power (150 mW) at which the data shown in Fig. 6 were obtained.

sharp rise and fall edges. The time resolution of the setup was measured to be ~8 μs.

The fluorescence decays for the LAS-Yb fibers are shown in Fig. 7. Notice that the data shown were obtained after normalization of the fluorescence signals on the values registered at 10 μs after the pump switching off (zero times in the figures). Fiber samples' lengths of less than 2 cm were used in the experiments to avoid the contributions of unwanted amplified spontaneous emission (ASE) and reabsorption; the fluorescence signals were collected from lateral surface of fiber samples, at the point separated by approximately 5 mm from splice with the LD output fiber. Typical Yb^{3+} fluorescence decays presented in Fig. 7 have been obtained at pump power of 150 mW, i.e. above the pump saturating levels (<10 mW) characteristic for all the fibers.

It is seen that the LAS-Yb fibers all demonstrate a virtually single-exponential fluorescence decay, with a constant τ varying between 720 μs (YbLa-5) and 760–770 μs (YbLa-3 and YbLa-4); the residual sum was always better than $R^2 = 0.98$ at fitting the experimental dependences. The found values are comparable with those for standard silica based fibers and seem to promise laser applications. There was not detected any shorter decay component in the fluorescence kinetics, at least in the time range in excess of 10 μs (the setup resolution).

Unfortunately, our attempts to measure the fluorescence decay of VIS "cooperative" emission failed – in virtue of its extremely low power to be registered in the lateral configuration with the available equipment.

Figure 8 demonstrates the dependences of fluorescence lifetime τ and integrated near-IR (Yb^{3+}) fluorescence power on the launched pump power at 976 nm.

Both dependences' sets have been obtained after processing the data of measurements of the fluorescence kinetics with a photo-detector. Namely, for each fiber and for pump powers varied from 3 to 400 mW, we applied the described procedure to get the lifetimes τ (the results are shown in Fig. 8(b)). Simultaneously, we recorded the signal measured by the photo-detector (voltage) at the times just before switching off the LD driver, which, after normalization, gave us the fluorescence levels shown in Fig. 8(a). [This implies that the signals were normalized on the number of *fluorescing* Yb^{3+} centers, different for each fiber.] The necessity to conduct such experiments will become clear when reporting the results of measurements of the nonlinear transmission coefficient of the LAS-Yb fibers (see the next part) where we reveal the presence in them of *non-fluorescing* Yb^{3+}-related centers.

One can also see from Fig. 8(b) that the lifetime value τ is virtually the same for all three fibers and is independent of pump power.

Concerning the fluorescence power, it is seen from Fig. 8(a) that Yb^{3+}-related fluorescence has a very similar saturating character for all fibers. This means that saturating pump power, *Ps*, is measured by vastly the same value, around 4.5–5.0 mW (YbLa-5) and around 7.5–8.5 mW (YbLa-3 and YbLa-4) though the fibers are, remind, quite different regarding Yb^{3+} content. A slightly smaller *Ps* value for YbLa-5 fiber as compared to YbLa-3 and YbLa-4 ones is simply the result of smaller Yb^{3+} doped core of the former (refer to Fig. 2 and Table I). As a consequence, *viz.*, in virtue of almost constant lifetime and saturating pump power for the LAS-Yb fibers, their absorption and emission cross-sections (Yb^{3+} transitions) are concluded to be close, too. Thus, we can estimate the absorption cross-section σ_a at the 976-nm peak of Yb^{3+}, implying that *(i)* pump-light propagation in a fiber has a multimode character (the core-field overlap factors for pump are

nearly 1, see Table I) and *(ii)* at the pump power corresponding to Yb^{3+} fluorescence saturation (a plateau in Fig. 8(a)) an Yb^{3+} inversion factor is ~0.5. The found estimate, $\sigma_a = \sigma_e = 0.98 \times 10^{-20}$ cm^2 (σ_e is the emission cross-section) for YbLa-5 fiber having the lowest Yb^{3+} concentration is surely valid. However the use of the found value for the heavily doped fibers, YbLa-3 and YbLa-4, can be non-trusty since the above made assumption implied Yb^{3+} centers in these two to be *fluorescent* (and apparently *single*), which is not the case; see below. Let's meanwhile provide the obtained estimates for absorption-cross sections for fibers YbLa-3 and YbLa-4: 1.76×10^{-20} and 1.64×10^{-20} cm^2, respectively.

Summarizing, the fluorescent properties of the LAS-Yb fibers are dependent but slightly on Yb^{3+} content and only regarding the strength or weakness of "cooperative" VIS emission. Thus, one might propose that Yb^{3+} concentration effect, in this aspect, is weak. However, the situation needs a rectification after making insight to the other – nonlinear-optical properties – of the fibers.

C. Nonlinear-Optical Properties

Nonlinear-optical response of a rare-earth doped fiber can be generally of different kinds and can be addressed by various manners and using a variety of experimental techniques. According to the main purpose announced in the present study, an inspection of the effect of Yb^{3+} concentration upon optical properties of the LAS-Yb fibers is, apparently, the basic goal to be achieved by characterizing them in terms of the nonlinear transmission coefficient. This quantity contains the information about the resonant-absorption saturation properties under in-band pump-light action and, probably, about some other specific effects such as concentration quenching. The other thing of interest, when characterizing a rare-earth doped fiber's optical nonlinearity, is its nonlinear refractive index (NRI), having impact on versatile laser and amplifier applications. How the concentration effect, in our case of Yb^{3+} dopants, manifests itself in NRI under resonant pumping is under scope, too.

1) Nonlinear Transmission Coefficient: Experiments were performed in the arrangement where a tested fiber is pumped by the LD with fiber output through the fibered isolator. A piece of each fiber (YbLa-5, YbLa-3, or YbLa-4) was spliced with the isolator's fiber, in turn spliced with the LD's output fiber. The transmission coefficient T of this piece was calculated as $T = P_{out}/P_{in}$, where P_{in} and P_{out} are, correspondingly, the measured pump powers on input and output of the fiber. A set of dependences of transmission coefficient on launched pump power $T(P_{in})$ was obtained for the LAS-Yb fibers for a variety of sample lengths L. The experimentally measured dependences $T(P_{in}, L)$ are shown in Fig. 9(a)–(c).

It is seen that the dependences $T(P_{in})$ demonstrate the "bleaching" character, a clear appearance of the resonant-absorption saturation. The dependences $T(L)$ (compare the curves on each plot (a), (b), and (c) in Fig. 9 where arrows sketch an increase of fiber length L) have a predictable trend, given by interplay between the Yb^{3+} resonant absorption, Yb^{3+} ASE contribution, and depleting of pump power at propagating along the fiber length.

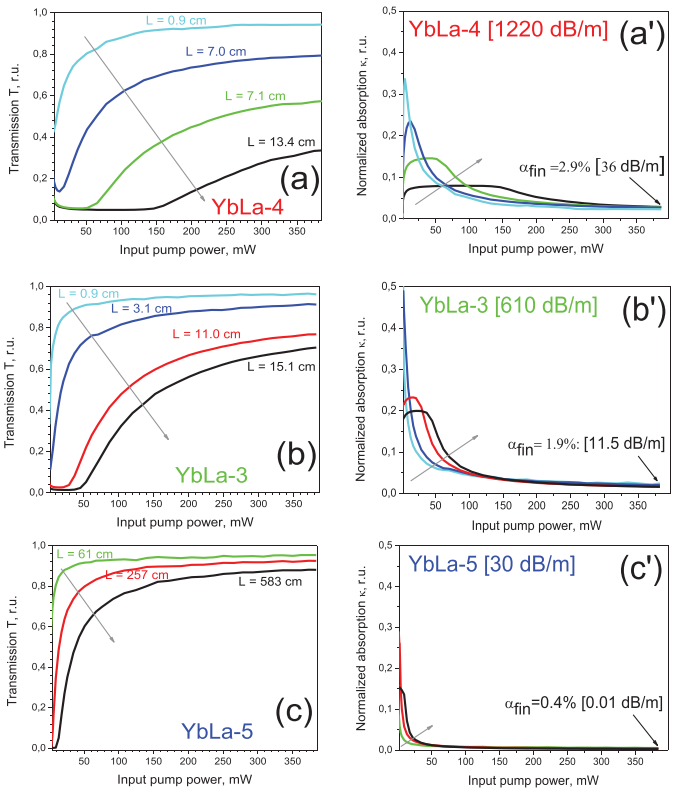

Fig. 9. Experimental dependences of nonlinear transmission coefficient T of fibers YbLa-4 (a), YbLa-3 (b), and YbLa-5 (c) (left column) and the correspondent dependences of normalized absorption coefficient κ (a', b', and c') on launched pump power P_{in} obtained for different lengths L of the fiber samples. Arrows show an increase of the fiber samples' length.

Making a simple transformation from the transmission (T) coefficients of the fibers, shown in the left-hand column of Fig. 9(a)–(c), to the normalized (on small-signal absorptions α_0, see Fig. 4) coefficients:

$$\kappa = -\ln(T)/L\alpha_0, \tag{1}$$

we obtain the results shown in the right-hand column of Fig. 9(a')–(c'). They show how the fibers' resonant (Yb^{3+}) absorption is saturated under the action of 976-nm pump. The two main observations can be made from these results: *(i)* There appear the plateau-like regions in the dependences κ (P_{in}), more and more "elongated" on P_{in} with increasing Yb^{3+} dopants' concentration, and *(ii)* the loss levels (they are marked by black arrows on the figures), where the dependences at increasing pump power approach, are essentially different for the fibers with different Yb^{3+} contents. Thus, the Yb^{3+} concentration effect appears here in much higher levels of pump powers, which are necessary for "bleaching" absorption, in fibers heavier doped with Yb^{3+}.

Apparently, certain contribution to this effect stems from trivial reabsorption (trapping) of light and migration of excitation among Yb^{3+} dopants, which is well-known; see e.g. Refs. [15]–[21]. However this process, at least in our case, cannot be associated with a decrease of lifetime of the excited state of *single* Yb^{3+} ions (see Fig. 6(d)) but should be instead

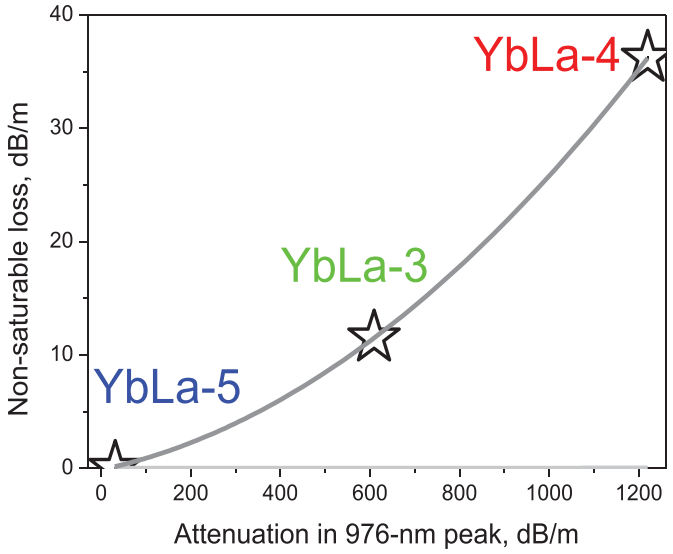

Fig. 10. Non-saturable loss in the LAS-Yb fiber as a function of attenuation in 976-nm peak of Yb^{3+}; the data were obtained from parts (a')–(c') of Fig. 9.

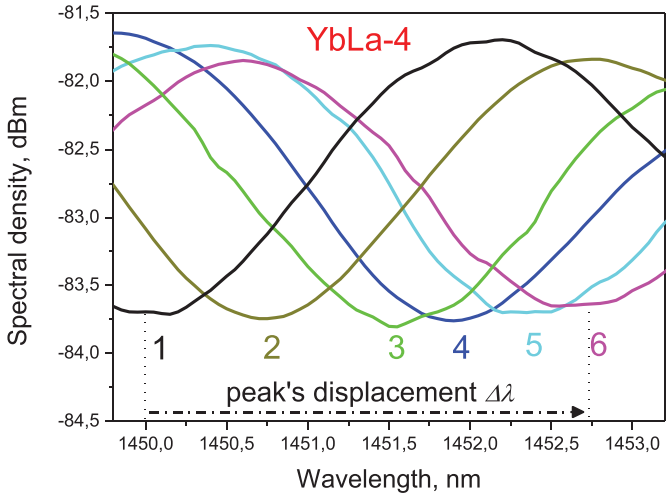

Fig. 11. Movement of spectral positions of the interferometer's fringes with an increase of pump power at 976 nm: curves 1, 2, 3, 4, 5, and 6 correspond to 0, 28, 65, 139, 211, and 281 mW. The data were obtained for YbLa-4 fiber with maximal Yb^{3+} concentration.

related to the existence of some species, most probably, Yb^{3+} *clusters*, having essentially different effective absorption at the pump wavelength and different relaxation time of excitation (see Section IV). On the other hand, an increase of non-saturable loss, at increasing Yb^{3+} concentration in the fibers is an additional evidence for such a conclusion. Let's remark here that the presence in heavily Yb doped fibers of intrinsic, virtually non-bleachable at in-peak (976 nm) pumping, "color" centers was detected long time ago [26]; however this fact until now did not get any doubtless explanation.

Another interesting feature seen from Fig. 9 is that full-saturated transmittance of the LAS-Yb fibers is always definitively less than 1, which points out the presence of nonlinear losses in them. Fitting the experimental dependences $T(P_{in}, L)$in Fig. 9(a)–(c) by a simple theory that implies the absorption saturation effect in the system of *single* Yb^{3+} ions but not accounts for any role of Yb^{3+} concentration (given by the presence of Yb^{3+} *clusters*; see the discussion below and e.g. Refs. [15]–[17], [20], [22]–[26]) was found to be incorrect. However it was not our aim here to make a precise modeling of the nonlinear transmission (absorption) coefficient of the fibers. Instead, a few important deductions, following from the data in Fig. 9 after simple algebraic transformations, can be made for clarifying the situation with the Yb^{3+} concentration effect regarding nonlinear absorption. As a resume, Fig. 10 helps one to capture the physical differences to appear between the low and the heavy doped LAS-Yb fibers in the sense of non-saturable loss. It is seen that an almost exponential increase of this loss is observed with increasing Yb^{3+} concentration (represented as usually in terms of attenuation in the 976-nm peak of Yb^{3+}). Undoubtedly, the featured by Fig. 10 facts ought to be reflected on operation of lasers implemented on the base of LAS-Yb fibers; see below.

2) NRI: The results of experiments from which we estimated NRI in the LAS-Yb fibers at 976 nm pumping are presented by Figs. 11–13.

There are known many approaches to estimate NRI in optical fibers [27]–[31]. We have employed the most reliable and at the same time simple method, where a fiber under study is placed between a couple of long-period fiber gratings (LPGs) forming a "modal" interferometer. We used the setup first proposed in Ref. [27], [28] so that the model developed there for estimating NRI is fully applicable to our case. The in-fiber interferometer is formed since the guided modes that propagate within a tested fiber's core interfere with the ones partially escaping (after the first LPG) and returning back (after the second LPG) to it. Spectral fringes at the output of the second LPG are observed by probing the fiber with low-power white light. The fringes occur due to a wavelength-dependent phase difference between the modes propagating through the fiber core and the ones propagating partially in the fiber cladding. Due to an expected nonlinearity of the tested fiber, the NRI of core area can be produced by launching high-intensity light into it, being the result of phase shifting between the two interfering modes. Thus, when the fiber placed inside the interferometer is subjected to the actions of high-intensity pump and low-intensity white light, one will observe a spectral shift of the interference fringes; such shift is related to the fiber's NRI, n_2, to be determined.

We used in experiments a pair of identical LPGs written in the conventional SMF-28 fiber with a spatial period of 400 μm; the LPGs were made to be optimal for the NRI measurements at 1.44 μm wavelength (i.e. spectrally aside the Yb^{3+} resonant band). The fringe patterns were obtained using low-power signal launched from the fibered white-light source at one side of the interferometer and detected at its opposite side, using OSA. The 400-mW LD was employed to pump the fiber under test from the side, opposite to launching white-light, achieved by splicing a 980/1550-nm WDM.

An example of how a chosen peak of the interference pattern suffers a spectral shift at increasing pump power is exemplified by Fig. 11, obtained for YbLa-4 fiber. From here, one can reveal a very strong pump-induced NRI in the fiber which is responsible for the fringes' spectral movement.

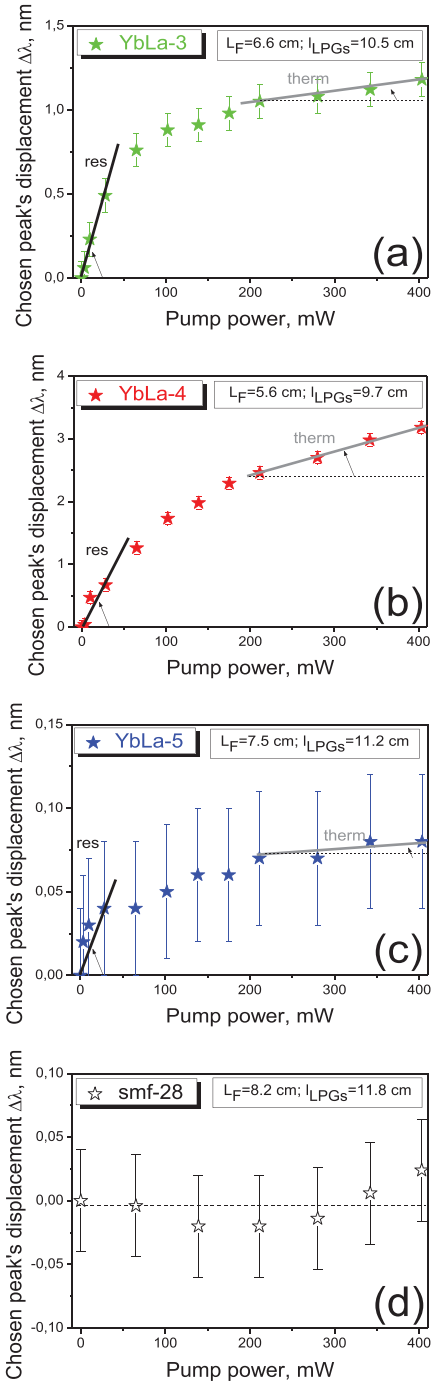

Fig. 12. Experimentally measured shifts of the interferometer pattern (displacement of a chosen fringe) as functions of pump power at 976 nm in the LAS-Yb fibers YbLa-3 (a), YbLa-4 (b), YbLa-5 (c), and in reference SMF-28 (d). The setup parameters are shown in the right top corners. Insets in each figure give the featuring interferometer's parameters. Solid lines guide the eye on the changes in the dependences at the lowest (mostly resonant NIRs) and highest (mostly thermal NIRs) pump powers.

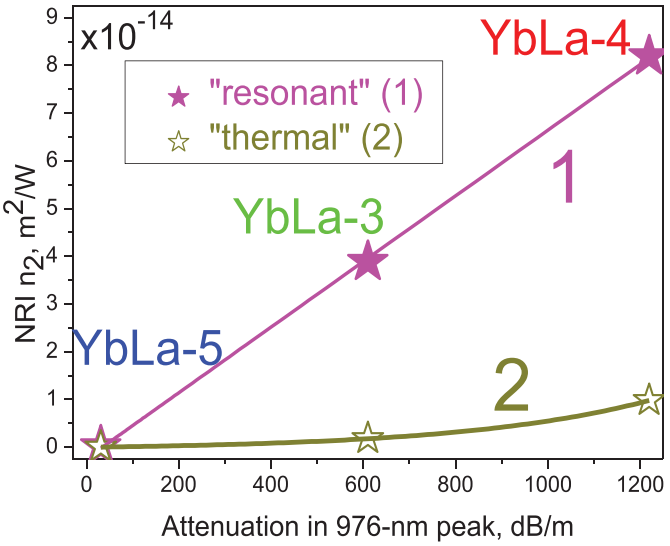

Fig. 13. The resonant (curve 1) and thermal (curve 2) NIR's contributions as functions of attenuation in 976-nm peak of Yb^{3+} in the LAS-Yb fibers, obtained from Fig. 12(a)–(c).

The whole set of the experimental results obtained for the LAS-Yb fibers are highlighted in Fig. 12(a)–(c) while Fig. 12(d) demonstrates the result of measurements with standard SMF-28 fiber as a reference. Note that due to the multimode propagation regime at around 1.44 μm in the LAS-Yb fibers, see Table I, the visibility of the interference pattern was worse than in SMF-28 (almost single-mode at this wavelength); however, this was not an obstacle to handle the experiments.

One can see from Fig. 12 that the fringes displacement notably increases in the LAS-Yb fibers with increasing pump power. Worth noticing is that the higher Yb^{3+} concentration in the fiber the larger is shift of the spectral fringes (compare plots (a)–(c)) and so the larger NRI. In the meantime for the SMF-28 fiber almost no change in the fringes' spectral positions was detected at increasing pump power; see Fig. 12(d). Core diameters of the LAS-Yb fibers (see Table I) differ small from core of SMF-28 fiber (8 μm); therefore NRI in these fibers arises due to the presence of Yb^{3+}. It should not be forgotten that the following estimates for NRI for the LAS-Yb fibers were made at 1.44 μm wavelength, whereas the NRI was "created" at the pump wavelength 976 nm, being associated with the Yb^{3+} resonant absorption saturation.

Given by the arrangement employed, the parameters used for estimating NRI in the LAS-Yb fibers are as it follows from Table II. In the Table, the parameters are: effective fiber's length L_{eff}, effective fiber's area A_{eff}; chosen peak's position λ_p; fringes spacing S; slope coefficient m, determined from a linear region of function $\Delta\lambda/P_p$ where $\Delta\lambda$ is the chosen peak's displacement and P_p is the pump power at 976 nm launched into the fiber. In Fig. 12(a)–(c) we show two such regions defined by m-value, which are marked by solid lines – for low and high pump powers, for each LAS-Yb fiber. One can calculate the NRI in a fiber using formula:

$$n_2 = \frac{A_{eff}\lambda_P}{2bL_{eff}S}\frac{\Delta\lambda}{P_P}, \tag{2}$$

where b is the polarization-dependent parameter between the pump and signal beams usually accepted to be equal to 2/3.

Using the fibers' parameters (see Tables I and II and Fig. 12), we can estimate NRI n_2. For the referent SMF-28 fiber we have obtained n_2 to be less than 5×10^{-19} m^2/W (a real value of n_2 for this fiber is below the method's resolu-

TABLE II
DATA USED AND OBTAINED AT NRI MODELING (LAS-Yb FIBERS)

Fiber ##	A_{eff} cm^2 $\times 10^{-7}$	L_{eff} cm	λ_p cm $\times 10^{-4}$	S cm $\times 10^{-7}$	Res. $\Delta\lambda/P_P$ cm/W $\times 10^{-6}$	Ther. $\Delta\lambda/P_p$ cm/W $\times 10^{-8}$	Res. n_2 m^2/W $\times 10^{-14}$	Ther. n_2 m^2/W $\times 10^{-14}$
YbLa-3	5.2	0.71	1.43	3.4	1.67	7.5	3.882	0.181
YbLa-4	4.6	0.36	1.45	4.3	2.51	30.1	8.191	0.982
YbLa-5	1.5	7.79	1.44	1.7	0.17	0.2	0.025	0.003

tion; therefore this estimate is not trusty). On the other hand, the n_2 values for the LAS-Yb fibers (see the last two columns in Table II) are reliable, being measured with accuracy given by the method's resolution (see the error bars in Fig. 12). It is seen that Yb^{3+} concentration strongly affects the NRI of the fibers like it does in the situations with other fiber properties, highlighted above. One can reveal from Fig. 12 that with increasing Yb^{3+} concentration not only a magnitude of the fringes' displacement dramatically increases but also a general behavior of the dependences in Fig. 12 (strongly different at high pump powers). The resonant NRI contribution, given by the presence of Yb^{3+} resonant transitions at the pump wavelength should be saturated at high pump powers, i.e. to approach some plateau; and it is indeed the case for low-doped YbLa-5 fiber. However the absence of such plateaus for heavily-doped YbLa-3 and especially YbLa-4 fibers forces us to think that certainly different, non-resonant, contribution in NRI n_2 should stand behind this.

As for us, notable heating of the heavily doped Yb^{3+} fibers, given by the presence in them of significant non-saturated loss can be an explanation. We found necessary to segregate these two contributions, "resonant" and "thermal", in NRI of the LAS-Yb fibers: See the last two columns in Table II and Fig. 13, revealing this side of the Yb^{3+} concentration effect.

It is seen from Fig. 13 that the dependence of the resonant NRI (curve 1) is almost linear on Yb^{3+} concentration (in terms of α_0), an expected trend given by the concentration dependence of the resonant polarizabilities of Yb^{3+} in the ground and excited states upon pumping. In the meantime, the behavior of the thermal NRI (curve 2) has a nonlinear on Yb^{3+} content character, most probably explained by nonlinear growth of non-saturable absorption and therefore by strong heating, associated with the presence of Yb^{3+} *clusters* in the fibers heavily doped with Yb^{3+}.

D. Laser and Photo-Darkening Tests

1) Laser Action: Laser experiments were implemented using the linear configuration of the cavity. A fiber sample was in-core pumped at 976 nm using the same LD and isolator. Pump light, after passing the isolator and a narrow-band (0.2 nm) fiber Bragg grating (FBG) with high reflectivity $R_1 = 99.9\%$ at 1080.6 nm, was delivered to the Yb doped fiber. The laser cavity was formed by this FBG and a perpendicularly cleaved end of the Yb doped fiber, having non-resonant Fresnel reflection ($R_2 = 3.5\%$). In experiments, different lengths of YbLa-3, YbLa-4, and YbLa-5 fibers were inspected.

It was found that output power of the lasers increases almost linearly with increasing pump power. Such dependences, for a few lengths of the LAS-Yb fibers, are exemplified in main frames of Fig. 14(a)–(c). It is seen that, for the adequately chosen optimal lengths given by the small-signal absorption coefficients' values (see Fig. 4), efficiency of lasing not exceeded 30% (overall) and 60% (slope). We didn't optimize the lasing efficiency by means of manipulations with reflectivity of FBGs' couplers, considering that the chosen values R_1 and R_2 permit the lasers operation at more-or-less beneficial, in terms of the pump-light absorption and output release, conditions. Threshold of lasing drastically rose with increasing length of the fibers (see Fig. 12) with a reasonable explanation being the presence of a part of non-saturated absorption, especially in heavily doped YbLa-3 and YbLa-4 fibers.

The optical spectra of lasers were found (see insets to Fig. 14(a)–(c)) to comprise a narrow-line of lasing (with bandwidth limited by 0.3 nm, defined mainly by the FBG spectral selectivity) and low-power ASE background. The ratio of spectrally integrated output within the laser line and within the broadband ASE in each case and for any pump power is of the order or less than 10^{-4}, revealing good spectral characteristics of the lasers in terms of the noise figure. Also notice a doublet shape of lasing at the use of YbLa-3 and YbLa-4 heavily-doped fibers, which seemingly originates from two orthogonal polarizations at self-induced pulsing in these cases. In contrast, a purely Lorentz spectrum was observed at the use of YbLa-5 low-doped fiber (the laser in this case operated in quasi-CW).

Interesting insight to unusual behavior of the lasers' thresholds is provided by Fig. 14(d) where we present the threshold values obtained for different lengths of YbLa-3, YbLa-4, and YbLa-5 fibers as functions of optical density $\alpha_0 L$ (the product of the fiber physical length and the absorption coefficient). It is seen that each of the dependences has a linear character when presented in double logarithmic scale, an expected trend. But a remarkable thing here is that their slopes are certainly different: The higher concentration of Yb^{3+} in the fiber the larger is slope, which is shown in inset to Fig. 14(d). Apparently, this could be solely caused by an increase of non-(or weakly) saturated loss at increasing Yb^{3+} concentration in the sequence YbLa-5$\rightarrow$YbLa-3$\rightarrow$YbLa-4.

However the most impressive differences between the LAS-Yb fibers having different Yb^{3+} contents can be seen from Fig. 15 where we highlight snapshots of oscillation at the lasers' outputs. The measurements were made using a photo-detector with bandwidth of 1.2 GHz.

The left, the middle, and the right columns in the figure show the oscillation regimes of lasers that were based,

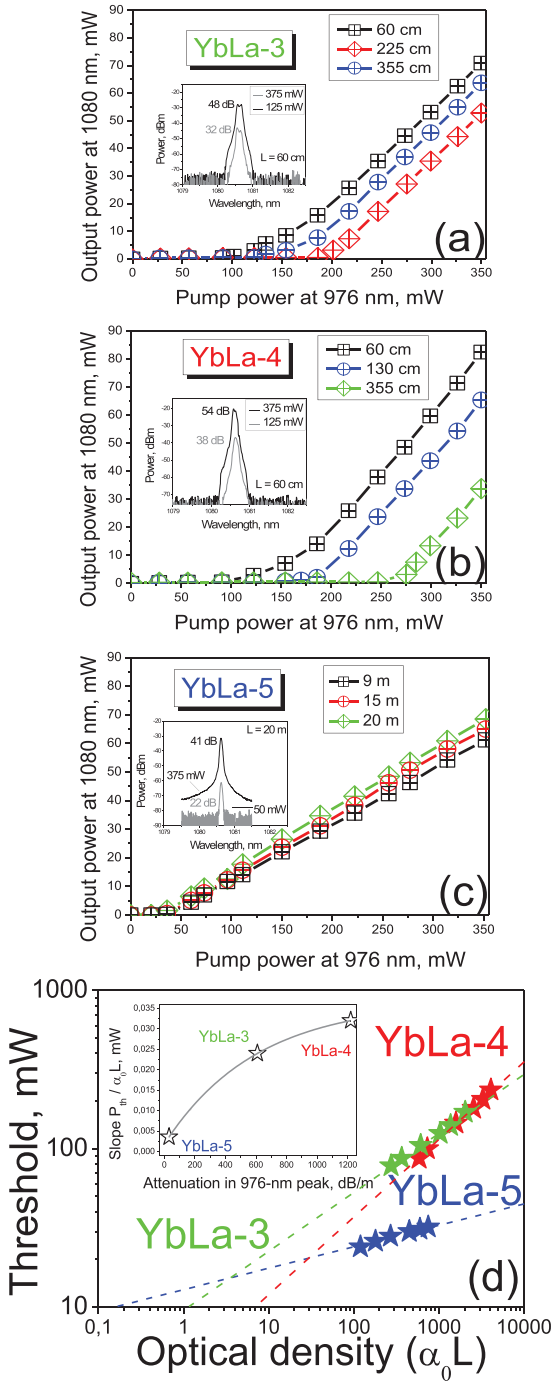

Fig. 14. Laser performances of the fiber lasers based on: (a) YbLa-3, (b) YbLa-4, and (c) YbLa-5 fibers, respectively. Insets in each plot show the lasers' optical spectra recorded near threshold (grey lines) and at maximal pump power (black lines) measured by OSA with 50-pm resolution. Each set of curves in the figures (a)–(c) corresponds to the set of lengths used, provided in the top-right corners. Thresholds of lasing as functions of LAS-Yb fibers' optical density $\alpha_0 L$ (d) as obtained from the generation curves in main frames of (a)–(c), where inset shows the dependence of slope of threshold versus attenuation in 976-nm peak of Yb^{3+}.

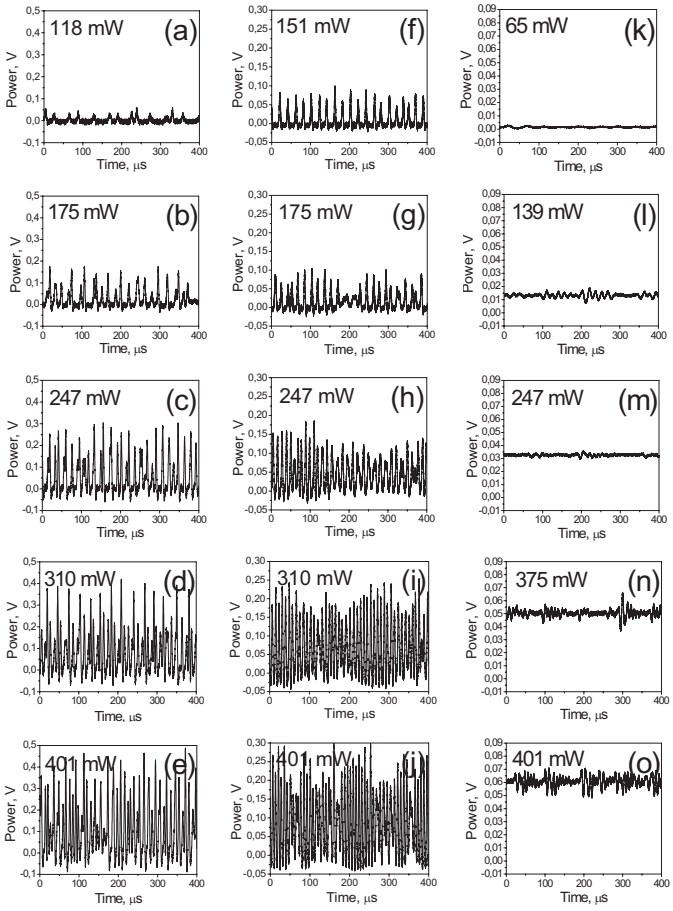

Fig. 15. Pump-power-dependent output spectra of lasers based on: (a)–(e) YbLa-4 fiber ($L = 60$ cm), (f)–(j) YbLa-3 ($L = 70$ cm); and (k)–(o) YbLa-5 ($L = 15$ m). Pump powers at which the snapshots were recorded are shown in the top-left corners.

correspondingly, on YbLa-4, YbLa-3, and YbLa-5 fibers. The regimes of the two first lasers – see traces (a)–(e) and (f)–(j), respectively – are essentially pulsed, with pulsing started up yet from thresholds; it is so-called self-Q-switching operation of an Yb doped fiber laser – see e.g. Refs. [32]–[34].

Notice that pulsing in the first two lasers has a merely irregular character, with one of possible reasons for that being the polarization beating, already mentioned. In contrast, the regimes of the third laser (see traces (k)–(o)) are seen to be almost pulsing-free (quasi-CW), although at increasing pump power there is a trend of the laser to get timing instabilities seen as stochastic "bursts" in the output.

Not entering in the physics that would stand behind these temporal irregularities, let's notice a clearly expressed trend to self-Q-switching at increasing concentration of Yb^{3+} dopants in the active fibers. An explanation for self-Q-switching can be the presence in the cavity of a "distributed" saturable absorber. A sole candidate for being a such-kind absorber is *clusters* of Yb^{3+} ions in the fibers. This could reasonably explain too different characters of lasing between the laser based on low-doped YbLa-5 fiber and the ones based on heavily-doped YbLa-3 and YbLa-4 fibers. In section IV, we provide some evidences for this.

Worth noticing, long-term inspection of output power of the laser based on YbLa-4 fiber has shown that it gradually dropped with time – by ~10%, depending on the pump level – after tens of minutes. Though the laser based on YbLa-3 fiber also demonstrated a similar trend, it was less expressed (in this case, output power decreased by about 5% after a few

hours of continuous operation). In contrast, the laser based on YbLa-5 fiber did not suffer at all from any degradation of output power. Apparently, this is a "signature" of the PD phenomenon, to be inspected as it follows.

2) Photodarkening Measurements: A few years ago, the pump-induced PD in Yb^{3+}-doped fibers has been recognized as the main drawback for power-scaling of Yb doped fiber lasers and amplifiers, especially in the case of using heavily doped fibers – see e.g. Refs. [14], [35]–[42]. Its detrimental appearance is the photo-induced loss, mainly in VIS but also tailing to near-IR spectral range, as the result of resonant (into Yb^{3+} band) pumping. This leads to deteriorating of output power of an Yb doped fiber system with operation time, sometimes measured by tens of percent.

Despite many sides of the PD phenomenon have been found thereafter – e.g. that magnitude of PD-induced loss in Yb doped fibers is proportional to the inversion level of Yb^{3+} ions and that degree of *clustering* of Yb^{3+} ions plays an important role in PD strength – a clear and doubtless explanation of the phenomenon is still absent. A variety of mechanisms to explain PD were proposed so far but the main question – why and how in-band (resonant) pumping of strongly shielded Yb^{3+} ions in Yb doped fibers could result in creating of color centers (with absorption spectrum being located in VIS) responsible for PD – is open. Also, it is not definitely clear why the PD phenomenon is more pronounceable in silicate Yb doped fibers than in phosphate ones.

The PD measurements were made at no lasing conditions, i.e. we used short pieces of LAS-Yb fibers without reflectors. The PD effect was treated by monitoring a fiber's attenuation spectra (using the white-light source as probe), measured after sequencing doses of irradiating at 976 nm wavelength. The spectra were recorded at the moments when pump light was temporally switched off. The LD output fiber was spliced to one of the input ports of a WDM (980/1550 nm) multiplexor and one of output ports of the latter was spliced to a piece of Yb doped fiber under test. Fiber output of the white-light source was spliced with this piece from opposite side and the transmitted light was, after passing WDM, analyzed using OSA, connected to the other WDM port. Thus, the pump and probe lights propagate in opposite directions in the fiber sample. The results are highlighted by Figs. 16–18.

From Fig. 16, it is seen that the LAS-Yb fibers suffer from PD by a different manner: the higher Yb^{3+} concentration the stronger PD is. Notice that pump power of 400 mW corresponded to an almost inverted system of Yb^{3+} ions, when around 50% of them are in the excited state (implying them *single*); see e.g. Fig. 8(a). Thus, the level of PD-induced loss strongly depends on Yb^{3+} concentration in the fibers. Note that the dependences shown in Fig. 16 are similar to the ones, well-known for PD of alumino-silicate fibers.

The results of PD experiments with YbLa-4 fiber, having the highest Yb^{3+} doping level (1220 dB/m) and so demonstrating the highest PD degree, are shown in Fig. 17.

It is seen from Fig. 17(a) that PD loss in VIS has not only different magnitudes but also different rates at different wavelengths and that PD strength depends significantly on

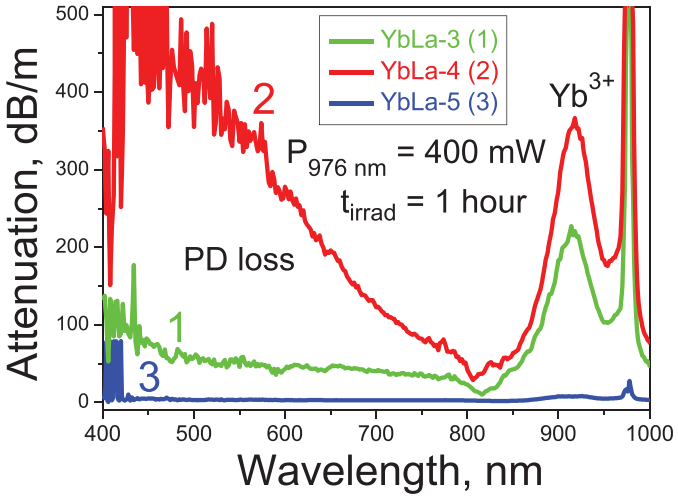

Fig. 16. Attenuation spectra of YbLa-3 (curve 1), YbLa-4 (curve 2), and YbLa-5 (curve 3) fibers after 1-h pumping at 976 nm (400 mW).

irradiation power. Similar but less pronounced features were observed for the less doped YbLa-3 fiber (not shown), whereas YbLa-5 fiber, having the lowest Yb^{3+} doping level, did not suffer from PD at all.

It should be noticed that the LAS-Yb fibers demonstrate a good resistance to PD if they are compared with standard, alumino-silicate fibers, being similar or even better in the sense of PD loss (see e.g. the recent papers [54], [55]). Seemingly, this is defined by enhancing impact of co-doping of the core glass with modifiers La and Li (see Section II) and also by the high content of Al_2O_3, a prerequisite for diminishing PD-induced loss in silica-based fibers [55].

Figure 17 (b) demonstrates the data of measurements of NRI in YbLa-4 fiber upon PD. The experiment has been conducted applying the technique, described in subsection C2. Pump power was kept in the experiment at the level of 400 mW, and shifting of the interferometer fringes during the fiber's irradiation was monitored. The maximal fringes displacement (around 0.25 nm) as the result of PD is negligible as compared with displacements arisen at changing the pump power (refer to Figs. 11 and 12(a)). Therefore the PD phenomenon virtually did not affect them when making the experiments on measurements of n_2.

Interestingly, the dynamics of PD loss during irradiation (Fig. 17(a)) essentially differs from the one of PD-induced NRI (Fig. 17(b)), a fact that probably demonstrates a complexity of the processes involved at PD, which needs a separate exploration.

Gathered together for all three LAS-Yb fibers (see Fig. 18), the results of PD tests allow one overview of what is appearance of the Yb^{3+} concentration effect in this case. Apparently, regarding PD of the fibers the Yb^{3+} concentration effect is mostly expressed as compared to the other fibers characteristics (see above). Therefore, PD seems to be stronger linked to Yb^{3+} dopants *clustering* in the fibers.

Note that the ratios of fully-saturated PD-induced loss levels at a wavelength 633 nm (usually taken for the characterization of PD strength in Yb doped fibers) to the small-signal absorption in the 976-nm peak of Yb^{3+}, were measured to

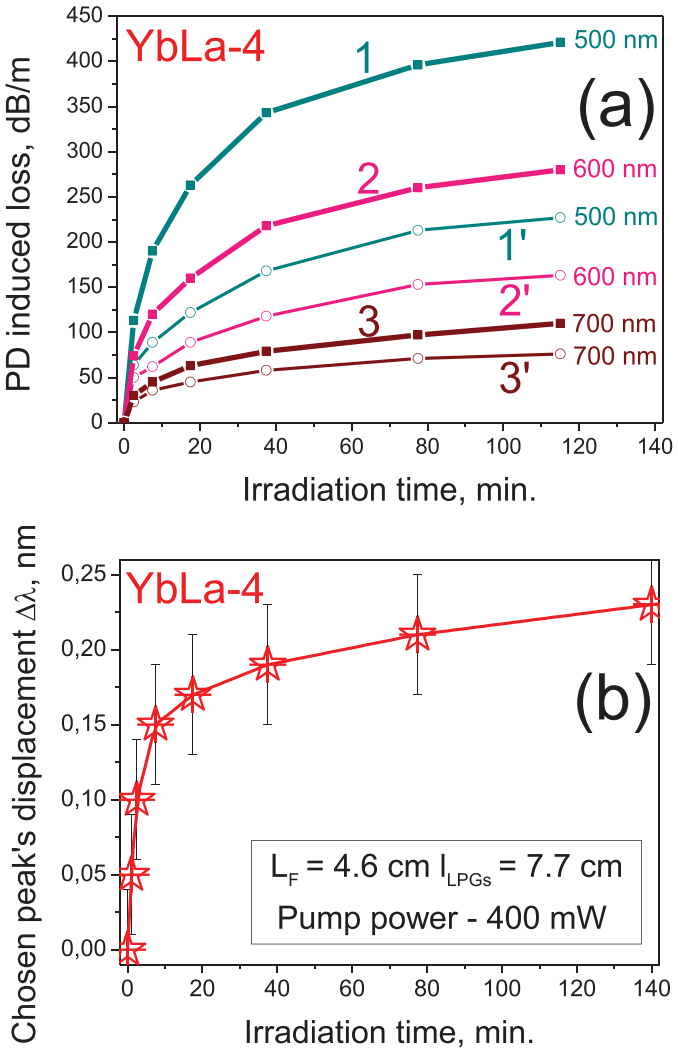

Fig. 17. (a) Dependences of PD-induced loss in YbLa-4 fiber versus irradiation time at pumping at 976 nm at pump levels of 100 mW (curves 1', 2', and 3') and 400 mW (curves 1, 2, and 3); curves 1, 2, and 3 and 1', 2', and 3' are obtained from the attenuation spectra, correspondingly, at wavelengths 500, 600, and 700 nm. (b) The correspondent PD-induced shifting of the interferometer pattern (displacement of a chosen fringe) as a function of irradiation time (measured at pump power of 400 mW). The setup parameters and calculated on NRI value are shown in the inset.

be 0.21 (YbLa-4), 0.07 (YbLa-3), and 0 (YbLa-5). Also note that Yb^{3+} fluorescence lifetime in PD-fibers was found to be almost not affected by PD (a vastly small decrease of lifetime which could be captured only for YbLa-4 fiber, but it was within the errors of fitting).

IV. Discussion

From the preceding analyses we can conclude that Yb^{3+} concentration has strong influence upon majority of optical properties of the LAS-Yb fibers. A hypothesis of what could be a reason for the consequences of an increase of Yb^{3+} concentration in these and probably in other heavily doped with Yb^{3+} silica fibers is highlighted below. [We emphasize here the hypothetical essence of the idea but we believe that it deserves announcing.]

Summarizing the data reported above, one can suppose that many of the trends revealed (from the spectra' measurements

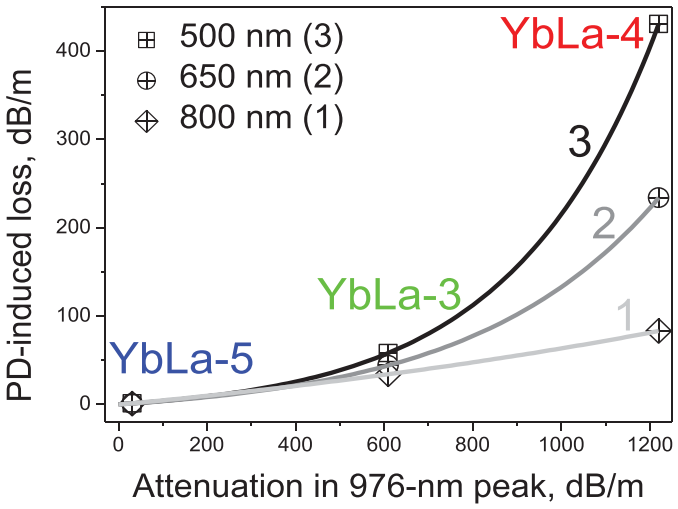

Fig. 18. PD excess loss in the LAS-Yb fibers as a function of attenuation in 976-nm peak of Yb^{3+} after 1-h pumping at 976 nm by pump power of 400 mW. Curves 1, 2, and 3 exemplify the PD loss measured at wavelengths 800 (curve 1), 650 (curve 2), and 500 (curve 3) nm.

to the PD data) originate from the changes in concentrations of Yb^{3+} ions and, seemingly, of other centers, closely related to them and spectrally matching them nearby 976 nm; see e.g. Refs. [26], [42], [43]. The experimental facts as the whole support the idea that *clustering* of the dopants (Yb^{3+} ions) is an important issue. The transformations of the whole of parameters affected by the concentration effect in the LAS-Yb fibers discussed above have a nonlinear on Yb^{3+} concentration character; see Figs. 6(d), 10, 13, 14, and 18. Most probably such *clusters* are composed of tightly coupled Yb^{3+} ions (*"chemical pairs"*). Apparently, some other "paired" complexes can also arise at increasing Yb^{3+} concentration, but we suggest here that Yb_2O_3 crystallites and their agglomerates can be present in the fibers with high content of Yb^{3+} ions [15]. Yb_2O_3 is one of sesquioxides, having a row of very interesting properties. For instance, it has a great absorption coefficient measured by about 300 cm^{-1} and short lifetime of the excited state of Yb^{3+} (around 10 μs), which is almost non-fluorescing. It is also known to have strong cooperative transitions and to be – at resonant 976-nm pumping – a source of broadband VIS-to-near-IR emission resulted from strong heating, see e.g. Refs. [44]–[46]. So, one may propose that certain areas of the fibers' core glass enriched by Yb_2O_3 crystallites, especially at high concentration of Yb^{3+} dopants, arise on the background of *single* Yb^{3+} ions "dissolved" in the glass [41], [48]. Yb^{3+} *clusters* in the form of inherent centers Yb_2O_3, absorption spectrum of which well matches the main absorption peak at 976 nm of dissolved single Yb^{3+} ions, seem to be relevant viewpoint on the matter. [Refer e.g. to Refs. [48], [49] where the presence of the strong 976-nm peak and vanishing of the 920-nm one was revealed to be characteristic for Yb_2O_3 while the peaks at 976 nm from *single* and *paired* Yb^{3+} are shown to match spectrally.]

One more argument can be considered, namely that Yb_2O_3 is a typical *defect* center in the core glass network, which can be formed at a high Yb^{3+} concentration. Probably, namely this "color" center, firstly detected yet in 1997

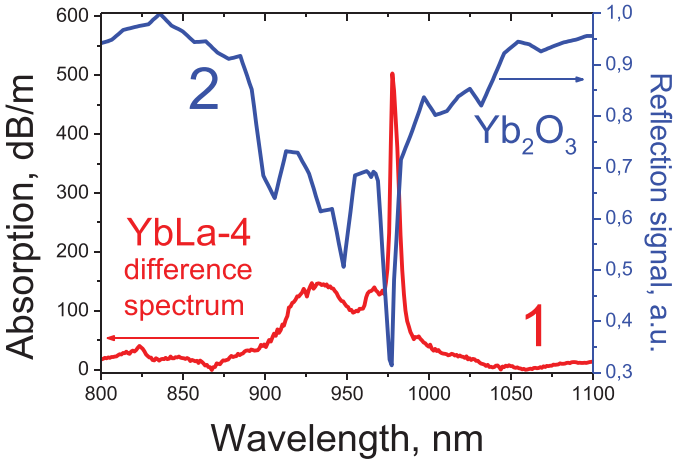

Fig. 19. Curve 1 — difference absorption spectrum obtained for YbLa-4 fiber after applying the fitting procedure described in the text; curve 2 – reflection spectrum of Yb_2O_3 powder.

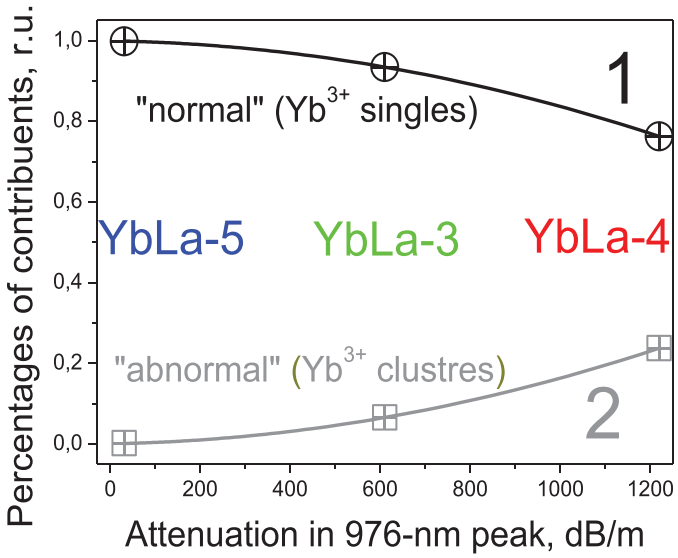

Fig. 20. Relative portions of "normal" absorption, assigned to Yb^{3+} single ions (curve 1) and "abnormal" one, assigned to Yb^{3+} paired complexes (Yb_2O_3). The data are obtained after modeling made for YbLa-3, YbLa-4, and YbLa-5 fibers, described in the text.

[26], is responsible for the presence of non-saturated (by 976-nm radiation) resonant absorption in heavily Yb^{3+} doped fibers [26], [50]–[53]. We recall here the results of the experiments where nonlinear transmission coefficient of the LAS-Yb fibers was measured and non-saturable absorption, strongly dependent on Yb^{3+} concentration, was revealed (see Fig. 10). This fact can be explained by extremely high absorption coefficient at 976 nm and almost quenched fluorescence, characteristic for Yb_2O_3 centers. Furthermore, possible presence of Yb_2O_3 centers in heavily Yb^{3+} doped fibers, which intensively absorb pump light but are non-fluorescent (quenched), may result in temperature rise in the core area, which seems to be a natural explanation for non-saturated character of NRI in the heavily-doped fibers YbLa-4 and YbLa-3 (see Fig. 13, curve 2). As well, self-Q-switching of lasers based on these fibers seems to be a closely related phenomenon.

It is logical to bridge here to the papers [43], [53] where the idea of an intrinsic "color" center, like Yb_2O_3, has been proposed to address some of the concentration phenomena in heavily rare-earth doped materials. Thus, the physical essences given by non-intentionally doping Yb doped fibers (in our case, LAS-Yb fibers) with Yb_2O_3 at high Yb^{3+} concentrations can be at least hypothesized. We have attempted to segregate a contribution that can be present in the absorption spectra of the heavily doped LAS-Yb fibers, YbLa-3 and YbLa-4, and cause the concentration-related spectral transformations, noticed in subsection IIIA. By making deconvolution of the absorption spectrum of YbLa-5 fiber (in which concentration of Yb^{3+} dopants is very low and thus no clustering is expected to occur) on Yb^{3+} subbands centered at 915–920, 976, and 1020 nm and approximating the original absorption spectra for YbLa-3 and YbLa-4 fibers by the found subbands, we have obtained the difference absorption spectra of these, YbLa-3 and YbLa-4, fibers. The resultant difference spectrum for YbLa-4 fiber is exemplified by curve 1 in Fig. 19.

It is seen that this spectrum demonstrates the features absent in "normal" absorption spectra of Yb^{3+} ions in silica glass, *viz.*, there are small-amplitude peaks usually met in absorption spectra of Yb^{3+} sesquioxide crystals (see e.g. Refs. [45], [46]) but not – in silica glass. Also notice that the most intensive absorption peak in curve 1 is very narrow and is slightly shifted to the Stokes side (to ~977 nm). The other thing is that the absolute value of the difference absorption coefficient in the main peak is about 500 dB/m, being a noticeable contribution in the overall peak extinction (1220 dB/m) of YbLa-4 fiber (see Fig. 4(a)).

We have also measured the reflection spectrum of chemically-pure powder of Yb_2O_3 oxide (see Ref. [44] for details) for making its direct comparison between the found difference absorption spectra of the LAS-Yb fibers. The reflection spectrum of Yb_2O_3 is shown in Fig. 19 by curve 2. One can see that these two (curves 1 and 2) demonstrate many similarities. We don't insist that such a comparison is worthy for evidencing the hypothesis about the presence of intrinsic Yb_2O_3 centers in the LAS-Yb fibers with high Yb^{3+} concentrations but we believe that this finding would be in its favor.

One more remark should be done regarding the estimates made in Section III when reporting Yb^{3+} absorption cross-sections σ_a at 976 nm for the LAS-Yb fibers. Remind that the values found from the saturation curves (Fig. 8) differed for the low-doped YbLa-5 fiber ($\sigma_a \sim 1\times10^{-20}$ cm^2) and heavily-doped YbLa-3 and YbLa-4 fibers ($\sigma_a \sim 1.7 \times 10^{-20}$ cm^2). Possible reason for the decline can be a considerable portion of Yb^{3+} ions, "joined" in Yb_2O_3 clusters in the last two fibers. The absorption cross-section of such inclusions is at least an order of value larger than the one of dissolved Yb^{3+} ions in glass (see above). Thus, the σ_a–values for YbLa-3 and (especially) YbLa-4 fibers seem to be overestimated because of a strong "Yb_2O_3 factor".

Before to conclude, let's give an illustration of how the difference absorptions found by the manner described above are related to the overall concentration of Yb^{3+} dopants. As usually, we imply that the last parameter, not known precisely (especially in fibers with high Yb^{3+} content) can be

attributed by extinction in the main Yb^{3+} peak at 976–977 nm. The result is shown in Fig. 20 where the data are provided for "normal" absorption (curve 1 in Fig. 20) [which is supposed to be assigned to *single* Yb^{3+} ions] and "abnormal" one (curve 2 in Fig. 20) [which is actually the difference absorption given by the rest of Yb^{3+} ions, hypothesized by us to be Yb_2O_3 centers]. It is seen that an increase of Yb^{3+} concentration in the fibers leads to a decrease in the number of the first contribuents (*single* Yb^{3+} ions) and an increase of the latter ones (Yb^{3+} ion *clusters*).

However, a more detailed research is definitively needed to confirm or reject the ideas proposed above.

V. Conclusion

Yb doped LAS based optical fibers with different concentrations of Yb^{3+} dopants have been fabricated through the conventional MCVD and SD processes.

The fibers have been thoroughly characterized first by means of absorption and fluorescence spectroscopy and lifetime measurements and then – applying the methods revealing the nonlinear-optical properties (nonlinear transmission and NRI); finally the fibers have been tested from the points of laser action and resistance to PD. In each of the applied characterization procedures, we focused on the features given by the effect of Yb^{3+} concentration in the fibers. Thereafter we could conclude on its significant impact upon virtually all the essential fibers' properties. In particular, we have detected notable transformations, as the appearance of the concentration effect, of the fibers' absorption spectra as well as its strong role at resonant (Yb^{3+}) absorption saturating and in NRI under the action of 976-nm pump. Also drastically an increase of Yb^{3+} concentration affects such a property of the LAS-Yb fibers as PD. An interesting aspect of Yb^{3+} concentration is its role in establishing of pulsed regimes in LAS-Yb based fiber lasers. At the same time, Yb^{3+} concentration has been recognized to weakly affect the near-IR fluorescence spectra and fluorescence lifetime, whereas it has definite influence upon strength of "cooperative" emission (in VIS). The higher Yb^{3+} concentration, the more pronounceable are e.g. the non-saturable absorption and NRI at in-band pumping, a trend to self-Q-switching of lasers based on the LAS-Yb fibers, and weakness to PD.

Thus, a full characterization of the fibers allows us to conclude that the effect of clustering of Yb^{3+} dopants stands behind the whole of the "concentration-dependent" features. The found laws forced us to propose that clustering of Yb^{3+} ions could itself have a specific character. We suggest a hypothesis that such type of Yb^{3+} clusters as simplest Yb_2O_3 crystallites can be responsible for the Yb^{3+} concentration-related effects in the fibers. Short distance between Yb^{3+} ions in such intrinsic clusters (which can lead to the "cooperative" fluorescence effects), extremely high absorption coefficient and short non-radiative lifetime of Yb_2O_3 (which can explain such features as the presence of weak or none absorption saturation at resonant pumping and, consequently, self-pulsing at laser action), as well as excessive thermal load (which allows to understand a high thermal contribution in NRI) – all these properties become understandable in attempt to address the effect of Yb^{3+} concentration in the fibers.

The fabricated fibers can be of interest for future basic studies, e.g. at revisiting the Yb^{3+} concentration-related effects discussed above, when dealing with Yb doped silica fibers with other core-glass hosts. On the other hand, LAS-Yb fibers can be also interesting for practical applications, if the concentration-dependent effects lightened above are negligible or weaken, which is ensured, as our estimates show, at absorption coefficient in the 976-nm peak of Yb^{3+} limited by 200–300 dB/m. A particular but important observation revealed for the LAS-Yb fibers, a good resistance to PD, deserves emphasizing. The LAS-Yb fibers have similar resistance to PD as compared with standard alumino-silicate Yb^{3+}-doped fibers with addition of P_2O_5, most probably thanks to the presence in the core glass of modifiers La and Li and the high doping level of Al_2O_3 [55] (remind that in the fabricated LAS-Yb fibers the phosphorous concentration is very small).

References

[1] A. V. Kir'yanov, M. C. Paul, Y. O. Barmenkov, S. Das, M. Pal, S. K. Bhadra, L. E. Zarate, and A. D. Guzman-Chavez, "Fabrication and characterization of new Yb-doped zirconia-germano-alumino silicate phase-separated nano-particles based fibers," *Opt. Exp.*, vol. 19, no. 16, pp. 14823–14837, 2011.

[2] M. C. Paul, M. Pal, A. V. Kir'yanov, S. Das, S. K. Bhadra, Y. O. Barmenkov, A. Martinez-Gamez, and J. L. Lucio-Martinez, "Yb-doped yttria-alumino-silicate nano-particles based optical fibers: Fabrication and characterization," *Opt. Laser Technol.*, vol. 44, no. 3, pp. 617–620, 2012.

[3] M. C. Paul, A. V. Kir'yanov, Y. O. Barmenkov, S. Das, M. Pal, S. K. Bhadra, S. Yoo, A. J. Boyland, J. K. Sahu, A. Martinez-Gamez, and J. L. Lucio-Martinez, "Yb_2O_3 doped yttrium-alumino-silicate nano-particles based LMA optical fibers for high-power fiber lasers," *J. Lightw. Technol.*, vol. 30, no. 13, pp. 2062–2068, Jul. 2012.

[4] P. Florian, N. Sadiki, D. Massiot, and J. P. Coutures, "27Al NMR study of the structure of lanthanum- and yttrium-based aluminosilicate glasses and melts," *J. Phys. Chem. B*, vol. 111, no. 33, pp. 9747–9757, 2007.

[5] Q. Zhang, G. Chen, G. Zhang, J. Qiu, and D. Chen, "Spectroscopic properties of Ho^{3+}/Yb^{3+} codoped lanthanum aluminium germinate glasses with efficient energy transfer," *J. Appl. Phys.*, vol. 106, p. 113102, Feb. 2009.

[6] Q. Zhang, G. Chen, G. Zhang, J. Qiu, and D. Chen, "Infrared luminescence of Tm^{3+}/Yb^{3+} codoped lanthanum aluminium germinate glasses," *J. Appl. Phys.*, vol. 107, no. 2, pp. 023102-1–023102-6, 2010.

[7] S. Balaji, A. D. Sontakke, and K. Annapurna, "Yb^{3+} ion concentration effects on 1 μm emission in tellurite glass," *J. Opt. Soc. Amer. B*, vol. 29, no. 7, pp. 1569–1579, 2012.

[8] M. J. Dejneka, B. Z. Hanson, S. G. Grigler, L. A. Zenteno, J. D. Minelly, D. C. Allan, W. J. Miller, and D. Kuksenkov, "Al_2O_3-La_2O_3-SiO_2 glasses for high-power, Yb^{3+}-doped, 980-nm lasers," *Glass Opt. Mater.*, vol. 85, no. 5, pp. 1100–1106, 2002.

[9] S. K. Singh, A. K. Singh, D. Kumar, O. Prakash, and S. B. Rai, "Efficient UV-visible up-conversion emission in Er^{3+}/Yb^{3+} co-doped La_2O_3 nano-crystalline phosphor," *Appl. Phys. B*, vol. 98, no. 1, pp. 173–179, 2010.

[10] F. Galakhov, B. Gorovaya, E. Demskaya, and T. Prokhorova, "Metastable liquid-phase separation in the Nd_2O_3-Al_2O_3-SiO_2 system," *Fiz. Khim. Stekla*, vol. 6, no. 1, pp. 46–50, 1980.

[11] M. Young, "Optical fiber index profiles by the refracted-ray method (refracted near-field scanning)," *Appl. Opt.*, vol. 20, no. 19, pp. 3415–3421, 1981.

[12] A. N. Trukhin, A. Sharakovski, J. Grube, and D. L. Griscom, "Sub-band-gap-excited luminescence of localized states in SiO_2-Si and SiO_2-Al glasses," *J. Non-Crystal. Solids*, vol. 356, nos. 20–22, pp. 982–986, 2010.

[13] V. F. Khopin, A. A. Umnikov, N. N. Vechkanov, A. E. Rozental', A. N. Gur'yanov, M. M. Bubnov, A. A. Rybaltovskii, A. V. Belov, and E. M. Dianov, "Effect of core glass composition on the optical properties of active fibers," *Inorg. Mater.*, vol. 41, no. 4, pp. 434–437, 2005.

[14] R. Peretti, C. Gonnet, and A. M. Jurdyc, "A new vision of photodarkening in Yb^{3+}-doped fibers," *Proc. SPIE*, vol. 8257, p. 825705, Feb. 2012.
[15] F. Auzel and P. Goldner, "Toward rare-earth clustering control in doped glasses," *Opt. Mater.*, vol. 16, nos. 1–2, pp. 93–103, 2001.
[16] P. Barua, E. H. Sekiya, K. Saito, and A. J. Ikushima, "Influences of Yb^{3+} ion concentration on the spectroscopic properties of silica glass," *J. Non-Cryst. Solids*, vol. 354, nos. 42–44, pp. 4760–4764, 2008.
[17] X. Zou and H. Toratani, "Evaluation of spectroscopic properties of Yb^{3+}-doped glasses," *Phys. Rev. B*, vol. 52, no. 22, pp. 15889–15897, 1995.
[18] P. D. Dragic, J. Ballato, T. Hawkins, and P. Foy, "Feasibility study of Yb:YAG-derived silicate fibers with large Yb content as gain media," *Opt. Mater.*, vol. 34, no. 8, pp. 1294–1298, 2012.
[19] Q. Zhang, J. Ding, B. Tang, J. Cheng, Y. Qiao, Q. Zhou, J. Qiu, Q. Chen, and D. Chen, "Optical properties of Yb^{3+} ions in SiO_2–Al_2O_3–CaF_2 glasses," *J. Phys. D, Appl. Phys.*, vol. 42, no. 23, p. 235405, 2009.
[20] N. Dai, L. Hu, and P. Lu, "Effects of Yb ion concentration on the spectral properties of lead silica glasses," *Opt. Commun.*, vol. 253, nos. 1–3, pp. 151–155, 2005.
[21] S. Guy, "Modelization of lifetime measurement in the presence of radiation trapping in solid-state materials," *Phys. Rev. B*, vol. 73, no. 14, pp. 144101-1–144101-8, 2006.
[22] S. Prucnal, L. Rebohle, and W. Skorupa, "Blue electroluminescence of ytterbium clusters in SiO_2 by co-operative up-conversion," *Appl. Phys. B*, vol. 98, nos. 2–3, pp. 451–454, 2010.
[23] L. R. P. Kassab, M. E. Fukumoto, V. D. D. Cacho, N. U. Wetter, and N. I. Morimoto, "Spectroscopic properties of Yb^{3+} doped PbO–Bi_2O_3–Ga_2O_3 glasses for IR laser applications," *Opt. Mater.*, vol. 27, no. 10, pp. 1576–1582, 2005.
[24] S. Ohara and Y. Kuroiwa, "Highly ytterbium-doped bismuth-oxide-based fiber," *Opt. Exp.*, vol. 17, no. 16, pp. 14104–14108, 2009.
[25] J. Y. Hu, H.-W. Yang, YJ. Chen, J. S. Lin, C. H. Lai, Y. M. Lee, and T. Zhang, "Properties and structure of Yb^{3+} doped zinc aluminum silicate phosphate glasses," *J. Non-Cryst. Solids*, vol. 357, nos. 11–13, pp. 2246–2250, 2011.
[26] R. Paschotta, J. Nilsson, R. Barber, E. Caplen, A. C. Tropper, and D. C. Hanna, "Lifetime quenching in Yb-doped fibres," *Opt. Commun.*, vol. 136, nos. 5–6, pp. 375–378, 1998.
[27] Y. H. Kim, B. H. Lee, Y. Chung, U. C. Paek, and W.-T. Han, "Resonant optical nonlinearity measurement of Yb^{3+}/Al^{3+} codoped optical fibers by use of a long-period fiber grating pair," *Opt. Lett.*, vol. 27, no. 8, pp. 580–582, 2002.
[28] A. Lin, B. H. Kim, D. S. Moon, Y. Chung, and W.-T. Han, "Cu^{2+}-doped germano-silicate glass fiber with high resonant nonlinearity," *Opt. Exp.*, vol. 15, no. 7, pp. 3665–3672, 2007.
[29] Y. O. Barmenkov, A. V. Kir'yanov, and M. V. Andres, "Resonant and thermal changes of refractive index in a heavily doped erbium fiber pumped at wavelength 980 nm," *Appl. Phys. Lett.*, vol. 85, no. 13, pp. 2488–2468, 2008.
[30] H. Garcia, A. M. Johnson, F. A. Oguama, and S. Trivedi, "Pump-induced nonlinear refractive-index change in erbium- and ytterbium-doped fibers: Theory and experiment," *Opt. Lett.*, vol. 30, no. 11, pp. 1261–1263, 2005.
[31] C. Ye, J. J. M. I. Ponsoda, A. Tervonen, and S. Honkanen, "Refractive index change in ytterbium-doped fibers induced by photodarkening and thermal bleaching," *Appl. Opt.*, vol. 49, no. 30, pp. 5799–5805, 2010.
[32] S. V. Chernikov, Y. Zhu, J. R. Taylor, and V. P. Gapontsev, "Supercontinuum self-Q-switched ytterbium fiber laser," *Opt. Lett.*, vol. 22, no. 5, pp. 298–300, 1997.
[33] D. A. Grukh, A. S. Kurkov, I. M. Razdobreev, and A. A. Fotiadi, "Self-Q-switched ytterbium-doped cladding-pumped fibre laser," *Quantum Electron.*, vol. 32, no. 11, pp. 1017–1019, 2002.
[34] A. V. Kir'yanov and Y. O. Barmenkov, "Self-Q-switched ytterbium-doped all-fiber laser," *Laser Phys. Lett.*, vol. 3, no. 10, pp. 498–502, 2006.
[35] J. J. Koponen, M. J. Soderlund, H. J. Hoffman, and S. K. T. Tammela, "Measuring photodarkening from single-mode ytterbium doped silica fibers," *Opt. Exp.*, vol. 14, no. 24, pp. 11539–11544, 2006.
[36] S. Yoo, C. Basu, A. J. Boyland, C. Stone, J. Nilsson, J. K. Sahu, and D. Payne, "Photodarkening in Yb-doped aluminosilicate fibers induced by 488 nm irradiation," *Opt. Lett.*, vol. 32, no. 12, pp. 1626–1628, 2007.
[37] S. Jetschke, S. Unger, A. U. Ropke, and J. Kirchhof, "Photodarkening in Yb doped fibers: Experimental evidence of equilibrium states depending on the pump power," *Opt. Exp.*, vol. 15, no. 22, pp. 14838–14843, 2007.
[38] J. J. Koponen, M. J. Soderlund, H. J. Hoffman, D. A. Kliner, J. P. Koplow, and M. Hotoleanu, "Photodarkening rate in Yb-doped silica fibers," *Appl. Opt.*, vol. 47, no. 9, pp. 1247–1256, 2008.
[39] Y.-W. Lee, M. J. F. Digonnet, S. Sinha, K. E. Urbanek, and R. L. Byer, "High-power Yb^{3+}-doped phosphate fiber amplifier," *IEEE J. Sel. Topics Quantum Electron.*, vol. 15, no. 1, pp. 93–102, Jan. 2009.
[40] A. V. Shubin, M. V. Yashkov, M. A. Melkumov, S. A. Smirnov, I. A. Bufetov, and E. M. Dianov, "Photodarkening of aluminosilicate and phosphosilicate Yb-doped fibers," in *Proc. Eur. Conf. Lasers Electro-Opt., Int. Quantum Electron. Conf.*, 2007, p. 1.
[41] A. D. Guzman-Chavez, A. V. Kir'yanov, Y. O. Barmenkov, and N. N. Il'ichev, "Reversible photo-darkening and resonant photo bleaching of ytterbium-doped silica fiber at in-core 977-nm and 543-nm irradiation," *Laser Phys. Lett.*, vol. 4, no. 10, pp. 734–739, 2007.
[42] A. V. Kir'yanov, "Electron-irradiation and photo-excitation darkening and bleaching of Yb doped silica fibers: Comparison," *Opt. Photon. J.*, vol. 1, no. 4, pp. 155–166, 2011.
[43] F. Auzel, "A fundamental self-generated quenching center for lanthanide-doped high-purity solids," *J. Lumin.*, vol. 100, nos. 1–4, pp. 125–130, 2002.
[44] V. M. Marchenko, L. D. Iskhakova, A. V. Kir'yanov, V. M. Mashinsky, N. M. Karatun, and E. M. Sholokhov, "Luminescence and selective heat radiation of Yb_2O_3 upon the resonant and thermal laser excitation," *Laser Phys.*, vol. 22, no. 1, pp. 177–183, 2012.
[45] J. Schugar, E. I. Solomon, W. L. Cleveland, and L. Goodman, "Simultaneous pair electronic transitions in Yb_2O_3," *J. Amer. Chem. Soc.*, vol. 97, no. 22, pp. 6442–6450, 1975.
[46] M. A. Noginov, G. B. Loutts, C. S. Steward, B. D. Lucas, D. Fider, V. Peters, E. Mix, and G. Huber, "Spectroscopic study of Yb doped oxide crystals for intrinsic optical bistability," *J. Lumin.*, vol. 96, nos. 2–4, pp. 129–140, 2002.
[47] S. Yoo, C. Basu, A. J. Boyland, C. Sones, J. Nilsson, J. K. Sahu, and D. Payne, "Reply to comment on 'Photodarkening in Yb-doped aluminosilicate fibers induced by 488 nm irradiation'," *Opt. Lett.*, vol. 33, no. 11, pp. 1217–1218, 2008.
[48] F. Auzel and P. Goldner, "Toward rare-earth clustering control in doped glasses," *Opt. Mater.*, vol. 16, nos. 1–2, pp. 93–103, 2001.
[49] A. Lupei and V. Lupei, "RE^{3+} pairs in garnets and sesquioxides," *Opt. Mater.*, vol. 24, nos. 1–2, pp. 181–189, 2003.
[50] A. V. Kir'yanov, Y. O. Barmenkov, I. L. Martinez, A. S. Kurkov, and E. M. Dianov, "Cooperative luminescence and absorption in ytterbium-doped silica fiber and the fiber nonlinear transmission coefficient at $\lambda = 980$ nm with a regard to the ytterbium ion-pairs' effect," *Opt. Exp.*, vol. 14, no. 15, pp. 3981–3992, 2006.
[51] A. Iho, M. Soderlund, J. J. M. Ponsoda, J. Koponen, and S. Honkanen, "Modeling inversion in an ytterbium-doped fiber," *Proc. SPIE*, vol. 7212, p. 721209, Jan. 2009.
[52] M. P. Hehlen, N. J. Cockroft, T. R. Gosnell, and A. J. Bruce, "Spectroscopic properties of Er and Yb -doped soda-lime silicate and aluminosilicate glasses," *Phys. Rev.*, vol. 56, pp. 9302–9318, Feb. 1997.
[53] F. Auzel, "Upconversion and anti-Stokes processes with f and d ions in solids," *Chem. Rev.*, vol. 104, no. 1, pp. 139–173, 2004.
[54] H. Gebavi, S. Taccheo, D. Milanese, A. Monteville, O. Le Goffic, D. Landais, D. Mechin, D. Tregoat, B. Cadier, and T. Robin, "Temporal evolution and correlation between cooperative luminescence and photodarkening in ytterbium doped silica fibers," *Opt. Exp.*, vol. 19, no. 25, pp. 25077–25083, 2011.
[55] S. Jetschke, S. Unger, M. Leich, and J. Kirchhof, "Photodarkening kinetics as a function of Yb concentration and the role of Al codoping," *Appl. Opt.*, vol. 51, no. 32, pp. 7758–7764, 2012.

Alexander V. Kirýanov (M'08) received the M.Sc. degree from M.V. Lomonosov Moscow State University, Moscow, Russia, in 1986, and the Ph.D. degree in optics and laser physics from A.M. Prokhorov General Physics Institute, Russian Academy of Sciences, Moscow, in 1995. He was with A.M. Prokhorov General Physics Institute from 1987 to 1998. He has authored or co-authored more than 170 scientific papers and holds four patents. His current research interests include solid-state and fiber lasers and nonlinear optics of solid state and optical fibers. Since 1998, he has been a Research Professor with the Centro de Investigaciones en Optica (CIO), Guanajuato, Mexico. He is a National Researcher (SNI III) and regular member of the Mexican Academy of Sciences. He has been a Senior Member of the Optical Society of America since 2010.

Mukul Chandra Paul received the M.Sc. degree in inorganic chemistry from the Burdwan University, Bardhaman, India, in 1989, and the Ph.D. degree in the development of radiation-sensitive fibers for evaluation of their radiation response behavior from the Central Glass and Ceramic Research Institute (CSIR-CGCRI), Kolkata, India, in 2003. Since 1997, he has been a Research Scientist with the Fiber Optics and Photonics Division, CSIR-CGCRI. He has authored 90 articles in journals and conference proceedings as author or co-author and holds four U.S. patents on fabrication of rare-earth doped fibers. He is a member of the Optical Society of America (2008) and a Life member of the Material Research Society of India and the Indian Ceramic Society. His current research interests include the development of different specialty optical fibers from viewpoint of material science. Present activity involves development of different rare-earth doped fibers for using in amplifier and fiber lasers, PS fibers for writing FBGs, advanced rare-earth doped nano-engineered host based optical fibers for high power fiber lasers and up-conversion lasers.

Yuri O. Barmenkov received the Ph.D. degree in radio-physics and electronics from the Leningrad (St. Petersburg) State Technical University, Leningrad, Russia, in 1991. Since 1996, he has been a Research Professor with the Centro de Investigaciones en Optica (CIO), Guanajuato, Mexico. He is a National Researcher (SNI-III) in Mexico, and a regular member of the Mexican Academy of Sciences. He has authored or co-authored over 130 scientific papers and holds three patents. His current research interests include single-frequency, CW and Q-switched fiber lasers, fiber optic sensors, and nonlinear optics of optical fibers.

Shyamal Das received the B.E. and M.E. degrees in chemical engineering from Jadavpur University, Kolkata, India. He has nearly five years research experience in sol-gel processing. He joined the Fiber Optics and Photonics Division, Central Glass and Ceramic Research Institute, Kolkata, in 2006. Since 2006, he has been working on fabrication of radiation sensitive fiber, Erbium and Thulium doped fibers, large flattened mode fiber, and specialty optical fibers.

Mrinmay Pal received the Ph.D. degree on specialty Erbium-doped fibers for broad-band amplification and gain-flattened optical amplifiers for WDM network systems. He has worked on development of EDFA for CATV and DWDM applications with industrial collaboration. Currently, he is working on fiber laser and supercontinuum generation with the Central Glass and Ceramic Research Institute, Kolkata, India. He has authored or co-authored 20 scientific articles in journals and conference proceedings as author or co-author and holds two U.S. patents on fabrication of rare-earth doped fibers. His current research interests include the development of optical fiber amplifiers, lasers, and photonics crystal fiber. He has been a member of the Optical Society of America since 2006 and a Life member of the Optical Society of India.

Luis Escalante-Zarate is currently pursuing the Ph.D. degree with the Photonics Division, Centro de Investigaciones en Optica, Guanajuato, Mexico. His current research interests include nonlinear properties of optical fibers and fiber lasers.